IEEE Access
Multidisciplinary | Rapid Review | Open Access Journal

Received November 18, 2018, accepted December 5, 2018, date of publication December 10, 2018,
date of current version January 7, 2019.

Digital Object Identifier 10.1109/ACCESS.2018.2885826

Spectral Efficient Spatial Modulation Techniques

HANY S. HUSSEIN[1,2], (Member, IEEE), MOHAMED ELSAYED[3], (Student Member, IEEE), USAMA SAYED MOHAMED[4], (Member, IEEE), HAMADA ESMAIEL[2], (Member, IEEE), AND EHAB MAHMOUD MOHAMED[2,5], (Member, IEEE)

[1]Electrical Engineering Department, Faculty of Engineering, King Khalid University, Abha 61411, Saudi Arabia
[2]Electrical Engineering Department, Faculty of Engineering, Aswan University, Aswan 81542, Egypt
[3]Electrical Engineering Department, Faculty of Engineering, Sohag University, Sohag 82524, Egypt
[4]Electrical Engineering Department, Faculty of Engineering, Assiut University, Assiut 71515, Egypt
[5]Electrical Engineering Department, College of Engineering, Prince Sattam Bin Abdulaziz University, Wadi Addwasir 11991, Saudi Arabia

Corresponding author: Hany S. Hussein (hahussein@kku.edu.sa)

This work was supported by the National Telecom Regulatory Authority (NTRA) Egypt under project title "LTE/WiFi/WiGig Internetworking for Future 5G Cellular Networks."

ABSTRACT Space modulation techniques (SMTs) have emerged as promising candidates for spectral- and energy-efficient wireless communication systems since they strike a good balance among error performance, power efficiency, spectrum efficiency, and receiver complexity. In SMTs, the information is not only conveyed by the habitual M-ary signal constellations; rather, it is also conveyed by the indices of the transmit antennas. As such, the indices of the transmit antennas are harnessed in such a manner that they enhance the transmission efficiency compared with the other multiple-input multiple-output opponents. Despite their exceptional advantages, SMTs suffer from a major drawback, which lies in the logarithmic proportion between their achievable data rates and the number of transmit antennas. In this regard, the fully generalized spatial modulation (F-GSM) and the fully quadrature spatial modulation (F-QSM) are proposed in this paper in order to vanquish this controversial drawback. In F-GSM and F-QSM, the transmit antennas used for data transmission are varied from the state in which only one transmit antenna is activated to the state in which multiple/all transmit antennas are activated. Therefore, a linear relationship between the achievable data rates and the number of transmit antennas is acquired. Moreover, a novel mathematical framework for assessing the average bit error rate performance of different SMTs is delineated. The driven mathematical framework is considered as the first major attempt to generalize the analytical analysis of different SMTs. In addition, the receiver's computational complexity of the proposed schemes is obtained and analyzed in terms of the computational complexity of different SMTs. The simulation results substantiate the validity of the analytical analysis conducted throughout the paper, as they are very akin to the obtained analytical formulas.

INDEX TERMS MIMO, space modulation techniques (SMTs), index modulation (IM), SM, GSM, QSM, F-GSM, F-QSM, achievable data rate, energy efficiency, spectral efficiency, computational complexity.

I. INTRODUCTION

In the last few years, index modulation (IM) has experienced unprecedented development in both academia and industry. Unlike traditional modulation techniques, IM uses innovative methods to achieve high data rates [1], [2]. Therefore, IM has emerged as one of the promising candidates for fifth-generation (5G) wireless networks due to its appealing advantages in terms of energy efficiency (EE), spectrum efficiency (SE), and low hardware complexity [3], [4]. The concept of IM is widely utilized today to describe the family of modulation techniques that harnesses the other transmit entities (i.e., subcarrier indices and/or transmit antenna indices) to embed additional information. These modulation techniques have been explicitly highlighted after the amalgamation of the orthogonal frequency division multiplexing (OFDM) with IM [1], [2] and after the infancy of the pioneering work of space modulation techniques [5]–[27].

OFDM-IM is a multi-carrier transmission technique that has drawn great attention from communication experts in the last few years [28]. It employs unparalleled methods to embed additional information via the indices of the subcarriers [29]. In OFDM-IM, subcarriers are partitioned into groups of active and inactive subcarriers. The active subcarriers are utilized to carry the habitual data constellation symbols and

the indices of these active subcarriers are used to convey additional information [30], [31]. Activation and inactivation of the subcarriers introduce not only an improvement in the system capacity but also a tremendous reduction in the power consumption of OFDM-IM as it reduces the high peak-to-average-power ratio (PAPR) offered by the traditional OFDM system [32]. The prior perspectives urge OFDM-IM to be beneficially used in replacement of the OFDM system, particularly in 5G networks [29].

Before the application of IM in multicarrier techniques, IM was applied to multiple-input multiple-output (MIMO) systems. The application of IM in MIMO systems led to the infancy of the pioneering modulation techniques, which are termed today as space modulation techniques (SMTs). SMTs such as space shift keying (SSK) [5]–[7], spatial modulation (SM) [8]–[11], generalized space shift keying (GSSK) [12], [13], generalized spatial modulation (GSM) [14]–[17], quadrature space shift keying (QSSK) [18], quadrature spatial modulation (QSM) [18]–[21], generalized quadrature space shift keying (GQSSK) [22] and generalized quadrature spatial modulation (GQSM) [23] are promising MIMO techniques that have captured increasing interest in the last few years due to their superiority in terms of EE, SE, and system complexity compared to the other MIMO opponents [10], [33]. SMTs harness in a new fashion the random nature of the communication channel to embed an additional information. This is done by using a simple coding mechanism that creates a one-to-one mapping between the transmitted bits and the spatial positions of the transmit antennas [11]. Therefore, one or multiple transmit antenna(s) is/are selected to transmit the habitual data constellation symbols, and the index/indices of the transmit antenna(s) is/are considered another source of information. Furthermore, the antenna selection process eliminates the need to have multiple radio frequency (RF) chains on the transmitter side (TX), eliminates the need for the sought-after inter-antenna synchronization (IAS), and permits the use of low-complexity decoding algorithms on the receiver side (RX) [10], [11].

Despite their exceptional advantages, SMTs suffer from a major drawback, which is explicitly represented in the logarithmic proportion of their achievable data rates with the number of transmit antennas (N_t) [11], [18]. This completely contradicts with the conventional Vertical-Bell Laboratories Layered Space Time (V-BLAST) technique [34], [35], in which a linear proportionality between its achievable data rate and N_t is achieved. Hence, to attain the same data rate as V-BLAST, SMTs require larger values of N_t. Therefore, this drawback is considered the main challenging problem that impedes the actual prevalence of SMTs. Hence, innovative methods are sought in this paper to overcome this controversial drawback.

To the best of the authors' knowledge, there were no systematic studies in the literature concerning the major drawback of SMTs until the authors proposed the fully-generalized spatial modulation (F-GSM) and the fully-quadrature spatial modulation (F-QSM) [36]–[38]. F-GSM and the F-QSM are proposed specifically to vanquish the main drawback of SMTs. In F-GSM and F-QSM, variable sets of transmit antennas are used for data embedding. More specifically, the data are transmitted by using a number of transmit antennas, in which a single antenna is active or multiple/all antennas are active. Thus, a linear proportionality between the achievable data rates and N_t is acquired in the proposed schemes instead of the logarithmic proportionality ingrained in conventional SMTs.

Using variable number of transmit antennas for data embedding dose not contradict the fact of having a single RF chain on the TX side, since just one splitter is required to simultaneously route the transmitted data to the active transmit antennas.

The work presented in this paper is related to our previous work presented in [36]–[38], in which a comprehensive study involving the different SMTs is presented. Compared to the work presented in [36]–[38], in this paper, we develop a general mathematical framework with detailed derivations to assess the average bit error rate (ABER) performance of the different SMTs. In addition, a detailed analysis of the computational complexity of the different SMTs is considered. Furthermore, extensive simulations are conducted to assess the performance of the proposed F-GSM and F-QSM based on different simulation scenarios and using different system metrics.

Following the concepts outlined above, the major contributions of this paper can be summarized as follows:

- *The F-GSM and the F-QSM System Models:* Two space modulation techniques, termed F-GSM and F-QSM, are proposed. Unlike the different SMTs in which the attainable data rates logarithmically increase with the number of transmit antennas, the attainable data rates of the proposed schemes linearly increase with the number of transmit antennas. The key idea of the proposed schemes is to use a variable number of transmit antennas to emit information. In other words, the number of antennas used for data transmission varies from the state in which only one transmit antenna is activated to the state in which multiple/all transmit antennas are activated. Therefore, the proposed schemes violate the strict restriction on the achievable data rates of most SMTs by fulfilling a linear proportionality between their attainable data rate and the number of transmit antennas. The system models of the proposed schemes are presented, and their operating principles are investigated in detail.
- *General Mathematical Framework for SMTs:* A novel mathematical framework for assessing the ABER performance of the different SMTs is laid out thoroughly. To the best of the authors' knowledge, this framework is the first major attempt that generalizes the analytical analysis of different SMTs. As such, closed-form expressions for the ABER of the SM, GSM, QSM, F-GSM, and the F-QSM are derived in detail. Moreover,

extensive Monte-Carlo simulations are utilized to substantiate the validity of the derived formulas.

- *Computational Complexity Analysis:* The receiver's computational complexity of the proposed F-GSM and F-QSM is evaluated by determining the total number of real operations (TNRO) required at their maximum-likelihood (ML) decoders. Moreover, it is compared with the computational complexity of the other SMTs.

The reminder of this paper is structured as follows. Section II introduces the related work. Section III and Section IV address the system models of the fully-generalized spatial modulation and the fully-quadrature spatial modulation, respectively. The performance of the proposed schemes is mathematically analyzed in Section V. The simulation results are reported in Section VI, and finally, the paper is concluded in Section VII.

Notation: Throughout this paper, bold lower and uppercase symbols are used to represent vectors and matrices, respectively. $CN\left(\mu,\sigma_o^2\right)$ is used to represent the complex Gaussian distribution of any random variable (RV), with μ and σ_o^2 standing for the mean and the variance, respectively. $p_\Psi(\Psi)$ indicates the probability density function (PDF) of any random variable Ψ. The ceiling and floor operators are denoted by $\lceil\cdot\rceil$ and $\lfloor\cdot\rfloor$, respectively. The superscripts $(\cdot)^T(\cdot)^*$ and $(.)^H$ are used to denote the transpose, the complex conjugate, and the Hermitian transpose, respectively. $\log_a(.)$, $|.|$ and $\Re(.)$ refer to the logarithm with base a, the magnitude operator, and the real part of complex quantity, respectively. $\binom{n}{k}$ indicates the binomial coefficient of choosing n outcomes from k possibilities. Finally, $Q(.)$ and $\Gamma(.)$ are used to indicate the well-known $Q-$function and the gamma function, respectively.

II. RELATED WORK

Regarding the existent literature, the concept of SMTs is deemed as a subject of excessive research and development in the last few years. The simplest version of SMTs is SSK [5]–[7]. In SSK, the information is not embedded using the habitual amplitude/phase constellation symbols; rather, it is embedded using the index of transmit antenna. The ability to have no amplitude/phase elements to generate the data constellation symbols (e.g., no RF chains required), relaxes the hardware requirements on the TX side and reduces the detection complexity on the RX side. Therefore, the achievable data rate of the SSK is expressed as follows [5]–[7]:

$$R_{SSK} = log_2\left(N_t\right), \tag{1}$$

where N_t denotes the number of transmit antennas.

In SM [8]–[11], a single RF chain is required on the TX side to generate the habitual data constellation symbols. Therefore, the information is embedded by both the data symbol and the index of the transmit antenna. As such, SM achieves a higher achievable data rate than SSK, but at the expense of increasing the hardware requirements on the TX side. Therefore, the achievable data rate of the SM is given by [8]–[11]

$$R_{SM} = log_2\left(M\right) + log_2\left(N_t\right), \tag{2}$$

where M stands for the modulation order or the constellation size.

GSSK [12], [13] is analogous to SSK, in which there is no need to generate the habitual data constellation symbols. However, in GSSK, a set of transmit antennas are used to embed information. This is contrary to SSK, where a single transmit antenna is utilized to convey information. Hence, in GSSK, there is no need for RF chains on the TX side; however, a single RF splitter is required to route the transmitted data to the corresponding transmit antennas via RF switches. Therefore, the achievable data rate of the GSSK is expressed as follows [12], [13]

$$R_{GSSK} = \left\lfloor log_2\binom{N_t}{N_s}\right\rfloor, \tag{3}$$

where N_s, $\binom{\cdot}{\cdot}$, and $\lfloor\cdot\rfloor$ denote the number of active antennas, the binomial coefficient, and the floor operator, respectively.

The same idea as in GSSK was exploited with SM to introduce what is termed today as GSM [14]–[17]. In GSM, a single RF chain is required on the TX side to generate the habitual data constellation symbols. However, a constant arbitrary number of transmit antennas are activated to transmit the same data constellation symbol. Therefore, the information is embedded by the indices of the active antennas and the transmitted data symbol. Hence, GSM achieves a higher achievable data rate than SM by activating a higher number of transmit antennas. Therefore, the achievable data rate of the GSM can be expressed as follows [14]–[17]

$$R_{GSM} = log_2(M) + \left\lfloor log_2\binom{N_t}{N_u}\right\rfloor. \tag{4}$$

where N_u denotes the number of antennas activated for data transmission.

QSSK [18] is analogous to SSK and GSSK, in which no RF chains are required on TX side to generate the habitual data constellation symbols. However, in QSSK, two orthogonal RF carrier signals are emitted using two transmit antennas, and the indices of these antennas are harnessed to embed the information. Hence, QSSK doubles the achievable data rate of the SSK, but at the expense of doubling the required number of transmit antennas. Therefore, the achievable data rate of the QSSK is given by [18]

$$R_{QSSK} = 2log_2\left(N_t\right). \tag{5}$$

In QSM [18]–[21], a single RF chain with in-phase (I) and quadrature-phase (Q) paths is used on the TX side to generate the real and the imaginary parts of the data constellation symbol, respectively. The real part is then transmitted using a single antenna, and the imaginary part is transmitted by another one. Consequently, QSM can fulfill a higher achievable data rate than SM by expanding the constellation diagram into two

distinct orthogonal dimensions. Therefore, the achievable data rate of the QSM can be expressed as follows [18]–[21]:

$$R_{QSM} = log_2 (M) + 2log_2 (N_t) . \quad (6)$$

GQSSK [22] is analogous to SSK, GSSK, and QSSK, in which no RF chains are required on the TX side to generate the data constellation symbols. However, in GQSSK, a set of transmit antennas are activated to transmit the in-phase part of the carrier signal, and another set are activated to transmit the quadrature part. Hence, two RF switches are required to transmit the in-phase component, and another two RF switches are utilized to transmit the quadrature-phase component. Therefore, the achievable data rate of the GQSSK is given by [22]

$$R_{GQSSK} = 2 \left\lfloor log_2 \binom{N_t}{N_s} \right\rfloor . \quad (7)$$

GQSM [23] is similar to QSM, in which a single RF chain with in-phase (I) and quadrature-phase (Q) paths is required on the TX side to generate the real and the imaginary parts of the data constellation symbol, respectively. However, a set of transmit antennas are used to transmit the real part of the data symbol, and another set are used to transmit the imaginary part. Thus, the achievable data rate of the GQSM is expressed as follows [23]:

$$R_{GQSM} = log_2 (M) + 2 \left\lfloor log_2 \binom{N_t}{N_u} \right\rfloor . \quad (8)$$

Differential quadrature spatial modulation (DQSM) [24] is regarded today as one of the recent advances in the field of SMTs. In DQSM, differential modulation and demodulation processes are harnessed in an innovative manner to obviate the requirement of perfect channel knowledge on the RX side. More specifically, in DQSM, the real and imaginary parts of the data constellation symbol are transmitted by permutations of the active antennas. Moreover, the transmitted signals at any time instant depends on the previous data block in addition to the current data block. As such, the achievable data rate of the conventional DQSM for N_t time-slots can be expressed as follows [24]:

$$R_{DQSM} = N_t log_2 (M) + \lfloor log_2(N_t!) \rfloor \quad (9)$$

where $log_2 (N_t!)$ represents all the possible permutations of the transmit antennas, with (.)! denoting the factorial operator.

In [25], complex quadrature spatial modulation (CQSM) was introduced. CQSM increases the spectral efficiency of conventional QSM by transmitting two data constellation symbols via the same channel. The first data symbol is drawn from any signal constellation diagram, whereas the second data symbol is a rotated version of the first symbol. Therefore, the achievable data rate of the CQSM is given by [25]

$$R_{CQSM} = 2log_2 (M) + 2log_2 (N_t) . \quad (10)$$

The problem that results when both the data symbols are transmitted from the same transmit antenna was highlighted in [25]. As such, the improved complex quadrature spatial modulation (ICQSM) technique was developed in order to increase the minimum Euclidean distance (ED) between the data constellation symbols and consequently enhance the bit error rate (BER) performance of the CQSM.

Diversity enhanced-spatial modulation (DE-SM) [26] applies the concept of signal space diversity (SSD) to enhance the BER performance of spatial modulation systems. In particular, in DE-SM, two data constellation symbols are first interleaved and rotated by a certain angle. Subsequently, the in-phase component of the first data symbol and the quadrature-phase component of the second data symbol are transmitted in the first time-slot. The other in-phase and quadrature-phase components of both data symbols are then transmitted in the subsequent time-slot. Therefore, the achievable data rate of the DE-SM is expressed in a manner similar to the achievable data rate of the CQSM (10).

A promising bit-to-symbol mapping technique for SM multiple-input single-output (MISO) systems was introduced in [27] to enhance the diversity gain of SMTs. This is done by mapping bit blocks to symbols in a manner that minimizes the Hamming distance between the adjacent symbols. In particular, partial knowledge of the state of the channel is assumed on the TX side, and the channel's magnitude of the transmit antennas is used to map the antenna selection bits, whereas the channel's phase of the transmit antenna is used to map the signal modulation bits.

The aforementioned studies endorse the major drawback of most of the existing SMTs that restricts their achievable data rates to be logarithmically proportional to the number of transmit antennas, N_t.

III. FULLY-GENERALISED SPATIAL MODULATION

The system model of the proposed F-GSM is depicted in Fig. 1. As shown in the figure, the upcoming block of bits to be transmitted at any time instant is split into two distinct groups. The first group of bits embeds $log_2 (M)$ bits that are referred to as data bits. This group of bits is utilized to modulate a signal constellation symbol from a signal constellation diagram of an arbitrary *M-ary* quadrature amplitude modulation (*M-QAM*) or from any other signal constellation diagram. The second group of bits embeds $(N_t - 1)$ bits that are termed the spatial bits. This group of bits is used to select the antenna subset utilized to transmit the data constellation symbol. The antenna subsets in the F-GSM, are varied from the state in which only one transmit antenna is activated to the state in which multiple/all transmit antennas are activated. This totally contradicts the conventional SM and GSM approaches, in which a single transmit antenna is activated in SM case or a constant number of antennas are activated in the GSM case. Varying the number of transmit antennas in the antenna subsets enhances the realization of the communication channel, simplifies the process of differentiating between the multiple paths of the channel, and therefore mitigates the deterioration in the BER performance.

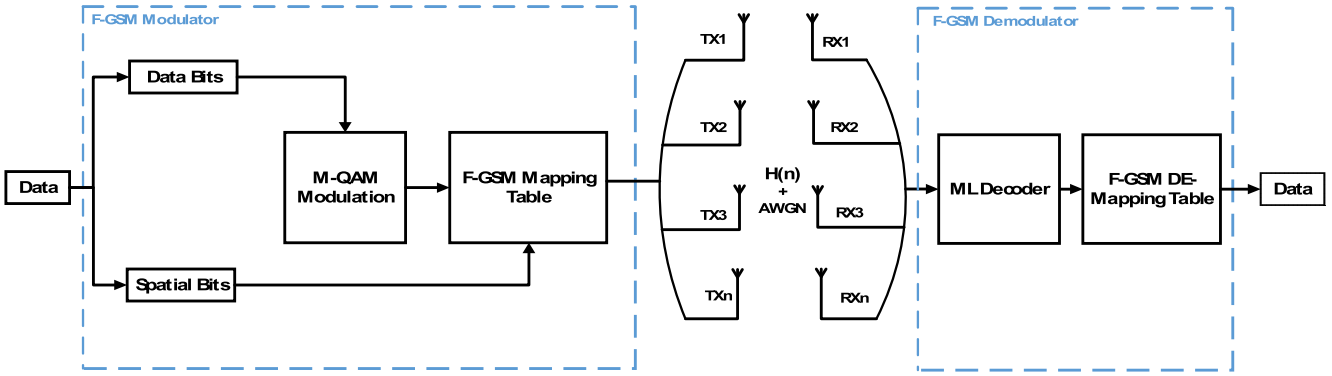

FIGURE 1. The Fully-Generalised Spatial Modulation System Model.

Therefore, the achievable data rate of the proposed F-GSM can be expressed as follows:

$$\begin{aligned} R_{F-GSM} &= log_2(M) + \left\lfloor \log_2\left(\sum_{k=1}^{N_t}\binom{N_t}{k}\right)\right\rfloor, \\ &= log_2(M) + \lfloor log_2(2^{N_t}-1)\rfloor, \\ &= \underbrace{log_2(M)}_{Data\ Bits} + \underbrace{(N_t-1)}_{Spatial\ Bits}, \end{aligned} \tag{11}$$

An example of the transmission principle of the proposed F-GSM is illustrated in Table 1. Herein, an SE of 5 bits per channel use (5 bpcu) is fulfilled by using 4 transmit antennas only. However, to achieve this SE, 8 transmit antennas are required in SM, and 5 transmit antennas (with $N_u = 3$) are required in GSM. Therefore, if the upcoming block of bits to be transmitted at any time instant is [$\underbrace{10}_{Data}$ $\underbrace{111}_{Spatial}$], the first group of bits [1 0] represents the data bits that modulate the data constellation symbol S. The second group of bits [1 1 1] represents the spatial bits that are used to map the data symbol S to the transmit antenna subset T_{x2} and T_{x3}.

TABLE 1. Example of F-GSM for 5 bpcu Transmission with $M = 4$ and $N_t = 4$.

Block of Bits		Transmitted Data			
Data Bits	Spatial Bits	T_{x1}	T_{x2}	T_{x3}	T_{x4}
b_1b_2	000	S	-	-	-
b_1b_2	001	-	S	-	-
b_1b_2	010	-	-	S	-
b_1b_2	011	-	-	-	S
b_1b_2	100	S	S	-	-
b_1b_2	101	S	-	S	-
b_1b_2	110	S	-	-	S
b_1b_2	111	-	S	S	-

As such, the resultant transmission vector of the proposed F-GSM $\boldsymbol{x} \in \mathbb{C}^{N_t\times 1}$ is $\boldsymbol{x} = [0\ S\ S\ 0]^T$. This vector is then transmitted over uncorrelated fading channel $\boldsymbol{H} \in \mathbb{C}^{N_r\times N_t}$ and experiences an additive white Gaussian noise (AWGN) $\boldsymbol{v} \in \mathbb{C}^{N_r\times 1}$ having independent Gaussian distributed real and imaginary parts and is expressed as $\boldsymbol{v} \sim \mathcal{CN}\left(0,\sigma_n^2\right)$, where N_r stands for the number of receive antennas.

Therefore, the received vector $\boldsymbol{y} \in \mathbb{C}^{N_r\times 1}$ on the RX side of the proposed F-GSM can be expressed as follows:

$$\boldsymbol{y} = \boldsymbol{h}_l S + \boldsymbol{v}, \tag{12}$$

and

$$\boldsymbol{h}_\ell = \sum_{i=1}^{N_u} \boldsymbol{h}_{li}, \tag{13}$$

where $\boldsymbol{h}_\ell$ stands for the summation of active antennas channel columns required to transmit the data symbol. $\boldsymbol{h}_{li}$ stands for the i^{th} columns of $\boldsymbol{H}$, and N_u denotes the number of transmit antennas that are chosen to transmit the same data symbol, which can be expressed as follows: $N_u = 1, 2, \ldots \left\lceil \frac{N_t}{2} \right\rceil$.

On the RX side, perfect knowledge of the channel state information (CSI) is assumed, as in [14] and [18], and an ML decoder is utilized to obtain the optimum performance of the proposed F-GSM. As such, the ML decoder of the proposed F-GSM can be expressed as follows:

$$\left[\tilde{\ell}, \tilde{S}\right] = \underset{l,s}{arg\ min} \|\boldsymbol{y} - \boldsymbol{h}_l S\|^2. \tag{14}$$

IV. FULLY-QUADRATURE SPATIAL MODULATION

In line with F-GSM, F-QSM employs the concept of varying the number of transmit antennas in the QSM instead of the GSM. The system model of the proposed F-QSM is depicted in Fig. 2. As shown in the figure, the upcoming block of bits to be transmitted at any time instant is split into three distinct groups. As in F-GSM, the first group of bits embeds $log_2(M)$ data bits, which are used to modulate a signal constellation symbol S from an arbitrary M-QAM constellation diagram. The data symbol S is then decomposed into its real and imaginary parts, ($S_{\Re}$) and ($S_{\Im}$), respectively, to be transmitted using one/multiple transmit antenna(s) depending on the subsequent group of bits. The second group of bits embeds $(N_t - 1)$ spatial bits. This group of bits is used to select the antenna subset required to transmit the real part of the data constellation symbol. Likewise, the third group of bits embeds $(N_t - 1)$ spatial bits, which are used to select the antenna subset required to transmit the imaginary part of

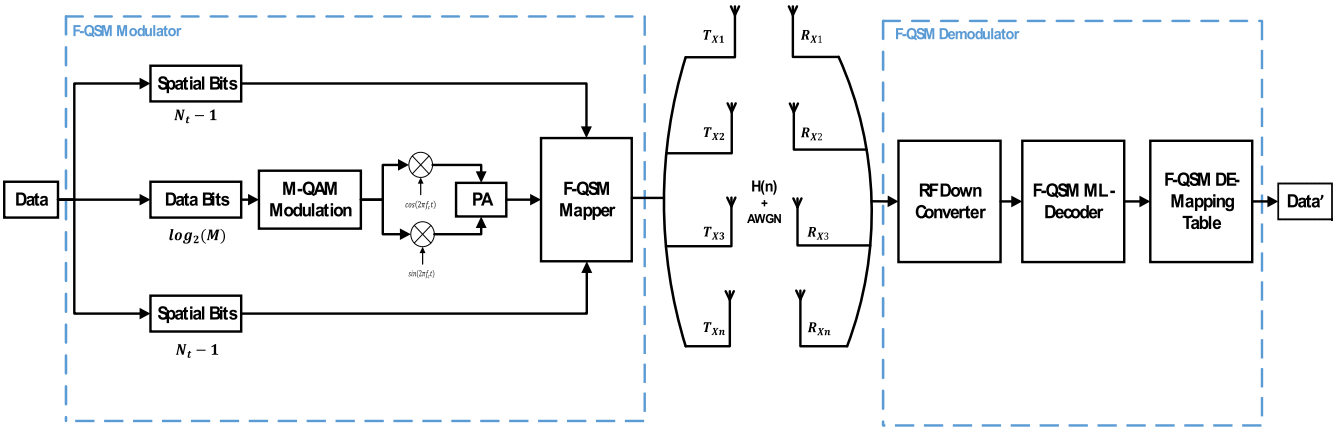

FIGURE 2. The Fully-Quadrature Spatial Modulation System Model.

the data symbol. Therefore, the achievable data rate of the proposed F-QSM can be expressed as follows:

$$\begin{aligned} R_{F-QSM} &= log_2(M) + \left\lfloor log_2\left(\sum_{k=1}^{N_t}\binom{N_t}{k}\right)\right\rfloor, \\ &= \underbrace{log_2(M)}_{Data\ Bits} + \underbrace{(N_t-1)}_{Spatial\ Bits}, \end{aligned} \tag{15}$$

An example of the transmission principle of the proposed F-QSM (for a certain block of bits) is illustrated in Table 2. Herein, an SE of 8 bpcu is fulfilled using 4 transmit antennas only. However, to maintain the same SE, 64 transmit antennas are required in SM, 8 transmit antennas (with $N_u = 4$) are required in GSM, and 8 transmit antennas are required in QSM.

TABLE 2. Example of F-QSM for 8 bpcu Transmission with $M = 4$ and $N_t = 4$.

Block of Bits		Transmitted Data			
Data Bits	Spatial Bits	T_{x1}	T_{x2}	T_{x3}	T_{x4}
b_1b_2	000000	S	-	-	-
b_1b_2	000001	$S_{\Re}$	$S_{\Im}$	-	-
b_1b_2	000010	$S_{\Re}$	-	$S_{\Im}$	-
b_1b_2	000011	$S_{\Re}$	-	-	$S_{\Im}$
b_1b_2	111100	$S_{\Im}$	S	$S_{\Re}$	-
b_1b_2	111101	$S_{\Im}$	$S_{\Re}$	S	-
b_1b_2	111110	$S_{\Im}$	$S_{\Re}$	$S_{\Re}$	$S_{\Im}$
b_1b_2	111111	-	S	S	-

Therefore, if the upcoming block of bits to be transmitted is [$\underbrace{11}_{Data}$ $\underbrace{111110}_{Spatial}$], the first group of bits [1 1] represents the data bits that modulate the data constellation symbol S. The data constellation symbol is then decomposed into its real $S_{\Re}$ and imaginary $S_{\Im}$ parts to be transmitted using one/multiple transmit antenna(s), depending on the subsequent group of bits. The second group of bits [1 1 1] represents the spatial bits that are used to map the real part of the data constellation symbol $S_{\Re}$ to the transmit antenna T_{x2} and T_{x3}. Likewise, the third group of bits [1 1 0] is used to map the imaginary part of the data constellation symbol $S_{\Im}$ to the transmit antennas T_{x1} and T_{x4}.

As such, the resultant transmission vector of F-QSM $\boldsymbol{x} \in \mathbb{C}^{N_t \times 1}$ is $\boldsymbol{x} = [jS_{\Im}\ S_{\Re}\ S_{\Re}\ jS_{\Im}]^T$. As in F-GSM, this vector is then transmitted over uncorrelated channel $\boldsymbol{H} \in \mathbb{C}^{N_r \times N_t}$ and experiences AWGN $\boldsymbol{v} \in \mathbb{C}^{N_r \times 1}$

Therefore, the received vector $\boldsymbol{y} \in \mathbb{C}^{N_r \times 1}$ on the RX side of the proposed F-QSM can be expressed as follows:

$$\boldsymbol{y} = \boldsymbol{h}_{\ell_{\Re}} S_{\Re} + j\boldsymbol{h}_{\ell_{\Im}} S_{\Im} + \boldsymbol{v}, \tag{16}$$

and

$$\boldsymbol{h}_{\ell_{\Re}} = \sum_{i=1}^{N_{\ell_{\Re}}} \boldsymbol{h}_{li}, \quad \boldsymbol{h}_{\ell_{\Im}} = \sum_{k=1}^{N_{\ell_{\Im}}} \boldsymbol{h}_{lk}, \tag{17}$$

where $\boldsymbol{h}_{\ell_{\Re}}$ and $\boldsymbol{h}_{\ell_{\Im}}$ represent the summation of active antennas channel columns required to transmit the real and imaginary parts of the data constellation symbol, respectively, and $\boldsymbol{N}_{\ell_{\Re}}, \boldsymbol{N}_{\ell_{\Im}} = 1, 2, \ldots\ldots \left\lceil \frac{N_t}{2} \right\rceil$.

As in F-GSM, an ML decoder is applied on the RX side to detect the antenna indices $\tilde{\ell}_{\Re}$ and $\tilde{\ell}_{\Im}$ along with the real and the imaginary parts of the data constellation symbol $\tilde{S}_{\Re}$ and $\tilde{S}_{\Im}$ as follows

$$\begin{aligned} &\left[\tilde{\boldsymbol{h}}_{\tilde{\ell}_{\Re}}, \tilde{\boldsymbol{h}}_{\tilde{\ell}_{\Im}}, \tilde{S}_{\Re}, \tilde{S}_{\Im}\right] \\ &\qquad = \arg \min_{\ell_{\Re}, \ell_{\Im}, S_{\Re}, S_{\Im}} \|\boldsymbol{Y} - \boldsymbol{h}_{\ell_{\Re}} S_{\Re} - j\boldsymbol{h}_{\ell_{\Im}} S_{\Im}\|^2. \end{aligned} \tag{18}$$

V. PERFORMANCE ANALYSIS

In this section, the performance of the proposed F-GSM and F-QSM is analyzed. First, a general mathematical framework for assessing the ABER of the various SMTs (e.g., SM, GSM, QSM, F-GSM, and F-QSM) is presented and deeply analyzed. Second, closed form expressions for evaluating the computational complexity of the proposed schemes are obtained and weighted against the computational complexity of the different SMTs.

A. ABER PERFORMANCE ANALYSIS

In SMTs, the ABER performance is evaluated using the well-known union bounding technique [39], [40] as follows:

$$ABER \leq \frac{1}{2^R}\sum_{n=1}^{2^R}\sum_{k=1}^{2^R}\frac{N\left(x_n \rightarrow \tilde{x}_k\right)p_r\left(x_n \rightarrow \tilde{x}_k\right)}{R}, \quad (19)$$

where $p_r\left(x_n \rightarrow \tilde{x}_k\right)$ is the pairwise error probability (PEP) when x_n is transmitted and $\tilde{x}_k$ is erroneously detected on the RX side. $N\left(x_n \rightarrow \tilde{x}_k\right)$ denotes the number of bits in error between x_n and $\tilde{x}_k$ and R denotes the rate of the transmitted bits However, the conditional pairwise error probability (C-PEP) can be expressed as follows:

$$p_r\left(x_n \rightarrow \tilde{x}_k \,|\, \boldsymbol{H}\right) = p_r\left(\|\boldsymbol{y} - \boldsymbol{h}_\ell S\|^2 > \|\boldsymbol{y} - \tilde{\boldsymbol{h}}_{\tilde{\ell}}\tilde{S}\|^2\right). \quad (20)$$

Using $\boldsymbol{y}$ as (12), the C-PEP can be reduced as follows:

$$p_r(x_n \rightarrow \tilde{x}_k|\boldsymbol{H}) = p_r(\|\boldsymbol{v}\|^2 > \|\boldsymbol{v} + \boldsymbol{h}_\ell S - \tilde{\boldsymbol{h}}_{\tilde{\ell}}\tilde{S}\|^2). \quad (21)$$

By letting $\boldsymbol{f} = \boldsymbol{e}_\ell S$, $\tilde{f} = \boldsymbol{e}_{\tilde{\ell}}\tilde{S}$ and expanding the norm operator, the right-hand side of (21) can be expressed as:

$$p_r\left(x_n \rightarrow \tilde{x}_k|\boldsymbol{H}\right) = p_r\left(\|\boldsymbol{v}\|^2 > \boldsymbol{v} + \boldsymbol{H}(\boldsymbol{f} - \tilde{f})\|^2\right) \quad (22)$$

where $\boldsymbol{e}_\ell$ and $\boldsymbol{e}_{\tilde{\ell}} \in \mathbb{R}^{N_t \times 1}$ are the columns of identity matrix $\boldsymbol{I}_{N_t \times N_r}$ Furthermore, if we let $\boldsymbol{g} = \left(\boldsymbol{f} - \tilde{f}\right)$, the C-PEP can be expressed as follows:

$$p_r\left(x_n \rightarrow \tilde{x}_k|\boldsymbol{H}\right) = p_r\left(-2\Re\left(\boldsymbol{v}^H\boldsymbol{H}\boldsymbol{g}\right)\boldsymbol{g}^H\boldsymbol{H}^H\boldsymbol{H}\boldsymbol{g}\right). \quad (23)$$

However, $\Re\left(\boldsymbol{v}^H\boldsymbol{H}\boldsymbol{g}\right)$ represents a Gaussian RV distributed as $\Re\left(\boldsymbol{v}^H\boldsymbol{H}\boldsymbol{g}\right) \sim (0, \frac{\sigma_n^2\boldsymbol{g}^H\boldsymbol{H}^H\boldsymbol{H}\boldsymbol{g}}{2})$. Therefore, the C-PEP can be expressed as follows:

$$p_r\left(x_n \rightarrow \tilde{x}_k \,|\, \boldsymbol{H}\right) = p_r\left(-2\sqrt{\frac{\sigma_n^2\boldsymbol{g}^H\boldsymbol{H}^H\boldsymbol{H}\boldsymbol{g}}{2}}\mathrm{u} > \boldsymbol{g}^H\boldsymbol{H}^H\boldsymbol{H}\boldsymbol{g}\right), \quad (24)$$

where u is a standard Gaussian RV.

However, the C-PEP (24) can be further reduced as follows:

$$p_r\left(x_n \rightarrow \tilde{x}_k \,|\, \boldsymbol{H}\right) = p_r\left(u > \sqrt{\frac{\boldsymbol{g}^H\boldsymbol{H}^H\boldsymbol{H}\boldsymbol{g}}{2\sigma_n^2}}\right), \quad (25)$$

$$p_r\left(x_n \rightarrow \tilde{x}_k \,|\, \boldsymbol{H}\right) = Q\left(\sqrt{\frac{\boldsymbol{g}^H\boldsymbol{H}^H\boldsymbol{H}\boldsymbol{g}}{2\sigma_n^2}}\right). \quad (26)$$

Therefore, the PEP can be expressed as follows:

$$p_r\left(x_n \rightarrow \tilde{x}_k\right) = E_H\left\{Q\left(\frac{\boldsymbol{q}^H\boldsymbol{q}}{2\sigma_n^2}\right)\right\}, \quad (27)$$

where $E_H\{.\}$ denotes the expectation over the fading channel $\boldsymbol{H}$ and $\boldsymbol{q}$ is expressed as follows:

$$\boldsymbol{q} = \boldsymbol{H}\boldsymbol{g} = \sum_{j=1}^{N_r}\boldsymbol{r}_j\boldsymbol{g}, \quad (28)$$

where $\boldsymbol{r}_j$ denotes the j^{th} row of the channel matrix $\boldsymbol{H}$.

The term $\boldsymbol{q}^H\boldsymbol{q}$ is chi-squared RV with $2N_r$ degree of freedom (DOF). Therefore, $\boldsymbol{q}^H\boldsymbol{q}$ can be rewritten as a function of a standard chi-squared RV Ψ as follows:

$$\boldsymbol{q}^H\boldsymbol{q} = \frac{\sigma_h^2\boldsymbol{g}^H\boldsymbol{g}}{2}\Psi, \quad (29)$$

However, the probability density function (PDF) of Ψ can be expressed as follows:

$$F\left(\Psi\right) = \begin{cases} \frac{\Psi^{N_r-1}e^{\frac{-\Psi}{2}}}{2^{N_r}\Gamma(N_r)} & \Psi > 0 \\ 0 & otherwise, \end{cases} \quad (30)$$

where $\Gamma\left(.\right)$ stands for the well-known gamma function. Using (27), (29), and (30), the PEP can be expressed as follows:

$$p_r\left(x_n \rightarrow \tilde{x}_k\right) = \int_0^\infty Q\left(\sqrt{\frac{\sigma_h^2\boldsymbol{g}^H\boldsymbol{g}\Psi}{4\sigma_n^2}}\right)\frac{\Psi^{N_r-1}e^{\frac{-\Psi}{2}}}{2^{N_r}\Gamma\left(N_r\right)}d\Psi. \quad (31)$$

The $Q-$function can be alternatively rewritten as follows [39]:

$$Q\left(x\right) = \frac{1}{\pi}\int_0^{\frac{\pi}{2}} e^{-\frac{x^2}{sin^2\theta}}d\theta. \quad (32)$$

As such, the PEP can be expressed as follows:

$$p_r\left(x_n \rightarrow \tilde{x}_k\right) = \frac{1}{2^{N_r}\pi\Gamma\left(N_r\right)} \times \int_0^{\frac{\pi}{2}}\int_0^\infty e^{-(\frac{1}{2}+\frac{B}{sin^2\theta})\Psi}\Psi^{N_r-1}d\theta d\Psi, \quad (33)$$

where $B = \frac{\sigma_h^2\boldsymbol{g}^H\boldsymbol{g}}{4\sigma_n^2}$. Define I_1 as

$$I_1 = \int_0^\infty e^{-\left(\frac{1}{2}+\frac{B}{sin^2\theta}\right)\Psi}\Psi^{N_r-1}d\Psi. \quad (34)$$

Then, $I_1(34)$ can be determined as in [39] and [40] as follows:

$$I_1 = \frac{2^{N_r}\Gamma\left(N_r\right)}{\left(\frac{sin^2\theta+B}{sin^2\theta}\right)^{N_r}}. \quad (35)$$

Substituting (35) in (33), the PEP can be given as follows:

$$p_r\left(x_n \rightarrow \tilde{x}_k\right) = \frac{1}{\pi}\int_0^{\frac{\pi}{2}}\left(\frac{sin^2\theta}{sin^2\theta + B}\right)^{N_r}d\theta. \quad (36)$$

However, the PEP (36) can be expressed as follows [39]:

$$p_r\left(x_n \rightarrow \tilde{x}_k\right) = \frac{1}{2}\left[1 - \mathfrak{U}\left(B\right)\sum_{k=0}^{N_r-1}\binom{2k}{k}\left(\frac{1-\mathfrak{U}^2\left(B\right)}{4}\right)^k\right], \quad (37)$$

where

$$\mathfrak{U}\left(B\right) = \sqrt{\frac{B}{1+B}}. \quad (38)$$

Moreover, (36) can be further rewritten as [40] as follows:

$$p_r\left(x_n \to \tilde{x}_k\right) = \left[\frac{1-\mathfrak{U}\left(B\right)}{2}\right]^{N_r} \sum_{k=0}^{N_r-1} \times \left(\frac{N_r-1+k}{k}\right)\left(\frac{1+\mathfrak{U}\left(B\right)}{2}\right)^{k}. \quad (39)$$

At high signal-to-noise ratios (SNRs), the pair-wise error probability provided by (37) and (39) can be rewritten in an asymptotic form using a Taylor series (TS) as follows [39], [40]:

$$p_r\left(x_n \to \tilde{x}_k\right) \simeq \left(\frac{1}{2}\right)\left(\frac{\Gamma\left(N_r+0.5\right)}{\sqrt{\pi}N_r!}\right)\left(\frac{1}{B}\right)^{N_r}. \quad (40)$$

It is worth mentioning here that the difference between the PEPs of the various SMTs mainly depends on B, which can be further rewritten as follows:

$$B = \frac{\sigma_h^2}{4\sigma_n^2}\eta, \quad (41)$$

where $\eta = \boldsymbol{g}^H\boldsymbol{g}$. However, η depends mainly on the data constellation symbols used in the transmission process of SMTs, and it can be determined for different SMTs as follows:

1) SPATIAL MODULATION

In the case of SM, η can be determined as follows [41], [42]:

$$\eta_{SM} = \begin{cases} \left|S-\tilde{S}\right|^2 & if\ \boldsymbol{h}_\ell = \tilde{\boldsymbol{h}}_{\tilde{\ell}} \\ |S|^2 + \left|\tilde{\boldsymbol{S}}\right|^2 & if\ \boldsymbol{h}_\ell \neq \tilde{\boldsymbol{h}}_{\tilde{\ell}}. \end{cases} \quad (42)$$

2) GENERALISED SPATIAL MODULATION

*Corollary 1:*In the case of GSM, Ψ can be expressed as

$$\eta_{GSM} = N_u\left|S-\tilde{S}\right|^2 + \Re\left(S\tilde{S}^*\right)\gamma\left(\ell,\tilde{\ell}\right), \quad (43)$$

where $\gamma\left(\ell,\tilde{\ell}\right)$ stands for the difference in the number of indices between ℓ and $\tilde{\ell}$. It should be noted here that η_{GSM}(43) has not yet been addressed in the literature, and it is introduced for the first time in this paper.

Proof: In conventional GSM, the difference in the number of indices between ℓ and $\tilde{\ell}$($i.e.\gamma\left(\ell,\tilde{\ell}\right)$) is restricted to be zero or even value. The rationale behinds this is that the number of transmit antennas chosen for data transmission ($i.e.N_u$) on the TX side of conventional GSM is always equal to the estimated number of transmit antennas that are detected at the ML decoder on the GSM RX side.

As such, the term η_{GSM} can be easily expressed as (43) by a precise auditing in a number of different examples for the transmission process of the conventional GSM as follows:

Example 1: when $N_t = 4$ and $N_u = 2$, the term η_{GSM} can be expressed as follows:

$$\eta_{GSM} = \begin{cases} 2\left|S-\tilde{S}\right|^2 & if\ \gamma\left(\ell,\tilde{\ell}\right)=0 \\ \left|S-\tilde{S}\right|^2 + |S|^2 + \left|\tilde{S}\right|^2 & if\ \gamma\left(\ell,\tilde{\ell}\right)=2 \\ 2\left(|S|^2 + \left|\tilde{S}\right|^2\right) & if\ \gamma\left(\ell,\tilde{\ell}\right)=4 \end{cases} \quad (44)$$

Example 2: when $N_t = 6$ and $N_u = 3$, the term η_{GSM} can be expressed as follows:

$$\eta_{GSM} = \begin{cases} 3\left|S-\tilde{S}\right|^2 & if\ \gamma\left(\ell,\tilde{\ell}\right)=0 \\ 2\left|S-\tilde{S}\right|^2 + |S|^2 + \left|\tilde{S}\right|^2 & if\ \gamma\left(\ell,\tilde{\ell}\right)=2 \\ \left|S-\tilde{S}\right|^2 + 2\left(|S|^2 + \left|\tilde{S}\right|^2\right) & if\ \gamma\left(\ell,\tilde{\ell}\right)=4 \\ 3\left(|S|^2 + \left|\tilde{S}\right|^2\right) & if\ \gamma\left(\ell,\tilde{\ell}\right)=6 \end{cases} \quad (45)$$

Example 3: when $N_t = 8$ and $N_u = 4$, the term η_{GSM} can be expressed as follows:

$$\eta_{GSM} = \begin{cases} 4\left|S-\tilde{S}\right|^2 & if\ \gamma\left(\ell,\tilde{\ell}\right)=0 \\ 3\left|S-\tilde{S}\right|^2 + |S|^2 + \left|\tilde{S}\right|^2 & if\ \gamma\left(\ell,\tilde{\ell}\right)=2 \\ 2\left|S-\tilde{S}\right|^2 + 2\left(|S|^2 + \left|\tilde{S}\right|^2\right) & if\ \gamma\left(\ell,\tilde{\ell}\right)=4 \\ \left|S-\tilde{S}\right|^2 + 3\left(|S|^2 + \left|\tilde{S}\right|^2\right) & if\ \gamma\left(\ell,\tilde{\ell}\right)=6 \\ 4\left(|S|^2 + \left|\tilde{S}\right|^2\right) & if\ \gamma\left(\ell,\tilde{\ell}\right)=8 \end{cases} \quad (46)$$

From the previous examples, η_{GSM} can be generalized as follows:

$$\eta_{GSM} = \left[\frac{2N_u - \gamma\left(\ell,\tilde{\ell}\right)}{2}\right]\left|S-\tilde{S}\right|^2 + \left[\frac{\gamma\left(\ell,\tilde{\ell}\right)}{2}\right]\left(|S|^2 + \left|\tilde{S}\right|^2\right). \quad (47)$$

Since $\left|S-\tilde{S}\right|^2 = |S|^2 - 2\Re\left(S\tilde{S}^*\right) + \left|\tilde{S}\right|^2$, η_{GSM} can be further reduced to obtain the formula in (43).

3) QUADRATURE SPATIAL MODULATION

For QSM, let $\boldsymbol{g} = \left(\boldsymbol{f}_{\ell_\Re} - \tilde{\boldsymbol{f}}_{\tilde{\ell}_\Re}\right) + j\left(\boldsymbol{f}_{\ell_\Im} - \tilde{\boldsymbol{f}}_{\tilde{\ell}_\Im}\right)$, with $\boldsymbol{f}_{\ell_\Re} = \boldsymbol{e}_{\ell_\Re} S_\Re, \boldsymbol{f}_{\ell_\Im} = \boldsymbol{e}_{\ell_\Im} S_\Im, \tilde{\boldsymbol{f}}_{\tilde{\ell}_\Re} = \boldsymbol{e}_{\tilde{\ell}_\Re} \tilde{S}_\Re, \tilde{\boldsymbol{f}}_{\tilde{\ell}_\Im} = \boldsymbol{e}_{\tilde{\ell}_\Im} \tilde{S}_\Im$ Therefore, η_{QSM} can be determined by a precise auditing in a number of different examples of the transmission process of QSM as in [18] and [42] as follows:

$$\eta_{QSM} = \begin{cases} \left|S_\Re - \tilde{S}_\Re\right|^2 + \left|S_\Im - \tilde{S}_\Im\right|^2 \\ \qquad \text{if } \boldsymbol{h}_{\ell_\Re} = \tilde{\boldsymbol{h}}_{\tilde{\ell}_\Re}, \quad \boldsymbol{h}_{\ell_\Im} = \tilde{\boldsymbol{h}}_{\tilde{\ell}_\Im} \\ |S_\Re|^2 + \left|\tilde{S}_\Re\right|^2 + |S_\Im|^2 + \left|\tilde{S}_\Im\right|^2 \\ \qquad \text{if } \boldsymbol{h}_{\ell_\Re} \neq \tilde{\boldsymbol{h}}_{\tilde{\ell}_\Re}, \quad \boldsymbol{h}_{\ell_\Im} \neq \tilde{\boldsymbol{h}}_{\tilde{\ell}_\Im} \\ \left|S_\Re - \tilde{S}_\Re\right|^2 + |S_\Im|^2 + \left|\tilde{S}_\Im\right|^2 \\ \qquad \text{if } \boldsymbol{h}_{\ell_\Re} = \tilde{\boldsymbol{h}}_{\tilde{\ell}_\Re}, \quad \boldsymbol{h}_{\ell_\Im} \neq \tilde{\boldsymbol{h}}_{\tilde{\ell}_\Im} \\ |S_\Re|^2 + \left|\tilde{S}_\Re\right|^2 + \left|S_\Im - \tilde{S}_\Im\right|^2 \\ \qquad \text{if } \boldsymbol{h}_{\ell_\Re} \neq \tilde{\boldsymbol{h}}_{\tilde{\ell}_\Re}, \quad \boldsymbol{h}_{\ell_\Im} = \tilde{\boldsymbol{h}}_{\tilde{\ell}_\Im} \end{cases} \tag{48}$$

4) FULLY-GENERALISED SPATIAL MODULATION

Corollary 2: In the proposed F-GSM, η_{F-GSM} can be expressed as (49), which is shown at the top of the next page. In this expression, $\tilde{N}_u$ denotes the number of transmit antennas that are estimated at the ML decoder of the F-GSM RX side.

Proof: Unlike GSM, the difference in the number of indices between 1 and $\tilde{\ell}$ can take any arbitrary value. The rationale behinds this is that the number of transmit antennas chosen for data transmission (*i.e.*, N_u) on the TX side of the proposed F-GSM is not necessarily equal to the estimated number of transmit antennas (*ie.*$\tilde{N}_u$) that are detected at the ML decoder on the F-GSM RX side.

As in conventional GSM, η_{F-GSM} can be simply determined by a precise auditing in a number of examples of the transmission process of the proposed F-GSM as follows:

Example 1: when $N_t = 5, N_u = 1$ and $\tilde{N}_u = 1$, the term η_{F-GSM} can be expressed as follows:

$$\eta_{F-GSM} = \begin{cases} \left|S - \tilde{S}\right|^2 & \text{if } \gamma\left(\ell, \tilde{\ell}\right) = 0 \\ |S|^2 + \left|\tilde{S}\right|^2 & \text{if } \gamma\left(\ell, \tilde{\ell}\right) = 2. \end{cases} \tag{50}$$

Example 2: when $N_t = 5, \quad N_u = 2$ and $\tilde{N}_u = 3$, the term η_{F-GSM} can be expressed as follows:

$$\eta_{F-GSM} = \begin{cases} 2\left|S - \tilde{S}\right|^2 + \left|\tilde{S}\right|^2 & \text{if } \gamma\left(\ell, \tilde{\ell}\right) = 1 \\ \left|S - \tilde{S}\right|^2 + |S|^2 + 2\left|\tilde{S}\right|^2 & \text{if } \gamma\left(\ell, \tilde{\ell}\right) = 3 \\ 2|S|^2 + 3\left|\tilde{S}\right|^2 & \text{if } \gamma\left(\ell, \tilde{\ell}\right) = 5. \end{cases} \tag{51}$$

Example 3: when $N_t = 5, \quad N_u = 2$ and $\tilde{N}_u = 2$, the term η_{F-GSM} can be expressed as follows:

$$\eta_{F-GSM} = \begin{cases} 2\left|S - \tilde{S}\right|^2 & \text{if } \gamma\left(\ell, \tilde{\ell}\right) = 0 \\ \left|S - \tilde{S}\right|^2 + |S|^2 + \left|\tilde{S}\right|^2 & \text{if } \gamma\left(\ell, \tilde{\ell}\right) = 2 \\ 2\left(|S|^2 + \left|\tilde{S}\right|^2\right) & \text{if } \gamma\left(\ell, \tilde{\ell}\right) = 4 \end{cases} \tag{52}$$

The previous examples clarify the concept of varying the number of transmit antennas of the proposed F-GSM. However, it is worth mentioning here that the proposed F-GSM approach includes the cases of SM (50) and GSM (52). Therefore, the conventional SM and GSM are considered as special cases of the proposed F-GSM method.

Following the above procedure, different examples of the transmission principle of the proposed F-GSM can be obtained and generalized to obtain the formula in (49), as shown at the bottom of this page.

5) FULLY-QUADRATURE SPATIAL MODULATION

Corollary 3: In F-QSM, η_{F-QSM} can be expressed as (53) which is illustrated at the top of the next page. In this expression, $N_{\ell_\Re}$ and $N_{\ell_\Im}$ denote the number of transmit antennas that are dedicated to transmit the real and imaginary parts of the data constellation symbols, respectively. Furthermore, $\tilde{N}_{\tilde{\ell}_\Re}$ and $\tilde{N}_{\tilde{\ell}_\Im}$ are the estimated number of antennas. $\gamma\left(\ell_\Re, \tilde{\ell}_\Re\right)$ and $\gamma\left(\ell_\Im, \tilde{\ell}_\Im\right)$ denote the difference in the number of indices between $\ell_\Re, \tilde{\ell}_\Re$ and $\ell_\Im, \tilde{\ell}_\Im$, respectively.

Proof: As in the F-GSM, the number of index difference between $\ell_\Re$ and $\tilde{\ell}_\Re$ or between $\ell_\Im$ and $\tilde{\ell}_\Im$ can take any arbitrary value. Since the number of transmit antennas chosen to transmit the real or the imaginary parts of the data symbol is not necessarily equal to the estimated number of antennas which is detected at the ML decoder of the F-QSM RX side.

$$\eta_{F-GSM} = \left[\frac{N_u + \tilde{N}_u - \gamma\left(\ell, \tilde{\ell}\right)}{2}\right]\left|S - \tilde{S}\right|^2 + \left[\frac{\gamma\left(\ell, \tilde{\ell}\right) + N_u - \tilde{N}_u}{2}\right]|S|^2 + \left[\frac{\gamma\left(\ell, \tilde{\ell}\right) - N_u + \tilde{N}_u}{2}\right]\left|\tilde{S}\right|^2 \tag{49}$$

$$\eta_{F-QSM} = \begin{cases} N_{\ell_\Re}\left|S_\Re - \tilde{S}_\Re\right|^2 + N_{\ell_\Im}\left|S_\Im - \tilde{S}_\Im\right|^2 & \text{if } \boldsymbol{h}_{\ell_\Re} = \tilde{\boldsymbol{h}}_{\tilde{\ell}_\Re}, \quad \boldsymbol{h}_{\ell_\Im} = \tilde{\boldsymbol{h}}_{\tilde{\ell}_\Im} \\ N_{\ell_\Re}\left|S_\Re - \tilde{S}_\Re\right|^2 + \left[\dfrac{N_{\ell_\Im} + \tilde{N}_{\tilde{\ell}_\Im} - \gamma\left(\ell_\Im, \tilde{\ell}_\Im\right)}{2}\right]\left|S_\Im - \tilde{S}_\Im\right|^2 + \left[\dfrac{v\left(\ell_\Im, \tilde{\ell}_\Im\right) + N_{\ell_\Im} - \tilde{N}_{\tilde{\ell}_\Im}}{2}\right]|S_\Im|^2 \\ \qquad + \left[\dfrac{\gamma\left(\ell_\Im, \tilde{\ell}_\Im\right) - N_{\ell_\Im} + \tilde{N}_{\tilde{\ell}_\Im}}{2}\right]\left|\tilde{S}_\Im\right|^2 & \text{if } \boldsymbol{h}_{\ell_\Re} = \tilde{\boldsymbol{h}}_{\tilde{\ell}_\Re}, \quad \boldsymbol{h}_{\ell_\Im} \neq \tilde{\boldsymbol{h}}_{\tilde{\ell}_\Im} \\ N_{\ell_\Im}\left|S_\Im - \tilde{S}_\Im\right|^2 + \left[\dfrac{N_{\ell_\Re} + \tilde{N}_{\tilde{\ell}_\Re} - \gamma\left(\ell_\Re, \tilde{\ell}_\Re\right)}{2}\right]\left|S_\Re - \tilde{S}_\Re\right|^2 + \left[\dfrac{\gamma\left(\ell_\Re, \tilde{\ell}_\Re\right) + N_{\ell_\Re} - \tilde{N}_{\tilde{\ell}_\Re}}{2}\right]|S_\Re|^2 \\ \qquad + \left[\dfrac{\gamma\left(\ell_\Re, \tilde{\ell}_\Re\right) - N_{\ell_\Re} + \tilde{N}_{\tilde{\ell}_\Re}}{2}\right]\left|\tilde{S}_\Re\right|^2 & \text{if } \boldsymbol{h}_{\ell_\Re} \neq \tilde{\boldsymbol{h}}_{\tilde{\ell}_\Re}, \quad \boldsymbol{h}_{\ell_\Im} = \tilde{\boldsymbol{h}}_{\tilde{\ell}_\Im} \\ \left[\dfrac{N_{\ell_\Re} + \tilde{N}_{\tilde{\ell}_\Re} - \gamma\left(\ell_\Re, \tilde{\ell}_\Re\right)}{2}\right]\left|S_\Re - \tilde{S}_\Re\right|^2 + \left[\dfrac{\gamma\left(\ell_\Re, \quad \tilde{\ell}_\Re\right) + N_{\ell_\Re} - \tilde{N}_{\tilde{\ell}_\Re}}{2}\right]|S_\Re|^2 \\ + \left[\dfrac{\gamma\left(\ell_\Re, \tilde{\ell}_\Re\right) - N_{\ell_\Re} + \tilde{N}_{\tilde{\ell}_\Re}}{2}\right]\left|\tilde{S}_\Re\right|^2 + \left[\dfrac{N_{\ell_\Im} + \tilde{N}_{\tilde{\ell}_\Im} - \gamma\left(\ell_\Im, \tilde{\ell}_\Im\right)}{2}\right]\left|S_\Im - \tilde{S}_\Im\right|^2 \\ + \left[\dfrac{\gamma\left(\ell_\Im, \tilde{\ell}_\Im\right) + N_{\ell_\Im} - \tilde{N}_{\tilde{\ell}_\Im}}{2}\right]|S_\Im|^2 + \left[\dfrac{\gamma\left(\ell_\Im, \tilde{\ell}_\Im\right) - N_{\ell_\Im} + \tilde{N}_{\tilde{\ell}_\Im}}{2}\right]\left|\tilde{S}_\Im\right|^2 & \text{if } \boldsymbol{h}_{\ell_\Re} \neq \tilde{\boldsymbol{h}}_{\tilde{\ell}_\Re}, \quad \boldsymbol{h}_{\ell_\Im} \neq \tilde{\boldsymbol{h}}_{\tilde{\ell}_\Im} \end{cases} \tag{53}$$

As such, η_{F-QSM} can be obtained by a precise auditing in number of examples of the transmission process of the proposed F-QSM as follows:

Example 1: when $N_t = 4$, $N_{\ell_\Re} = \tilde{N}_{\tilde{\ell}_\Re} = 1$ and $N_{\ell_\Im} = \tilde{N}_{\tilde{\ell}_\Im} = 1$, the term η_{F-QSM} can be expressed as QSM [18] as follows:

$$\eta_{F-QSM} = \begin{cases} \left|S_\Re - \tilde{S}_\Re\right|^2 + \left|S_\Im - \tilde{S}_\Im\right|^2 \\ \qquad \text{if } \gamma\left(\ell_\Re, \quad \tilde{\ell}_\Re\right) = 0, \ \gamma\left(\ell_\Im, \tilde{\ell}_\Im\right) = 0 \\ \left|S_\Re - \tilde{S}_\Re\right|^2 + |S_\Im|^2 + \left|\tilde{S}_\Im\right|^2 \\ \qquad \text{if } \gamma\left(\ell_\Re, \quad \tilde{\ell}_\Re\right) = 0, \ \gamma\left(\ell_\Im, \tilde{\ell}_\Im\right) = 2 \\ \left|S_\Im - \tilde{S}_\Im\right|^2 + |S_\Re|^2 + \left|\tilde{S}_\Re\right|^2 \\ \qquad \text{if } \gamma\left(\ell_\Re, \quad \tilde{\ell}_\Re\right) = 2, \ \gamma\left(\ell_\Im, \tilde{\ell}_\Im\right) = 0 \\ |S_\Re|^2 + \left|\tilde{S}_\Re\right|^2 + |S_\Im|^2 + \left|\tilde{S}_\Im\right|^2 \\ \qquad \text{if } \gamma\left(\ell_\Re, \quad \tilde{\ell}_\Re\right) = 2, \ \gamma\left(\ell_\Im, \tilde{\ell}_\Im\right) = 2 \end{cases} \tag{54}$$

Example 2: when $N_t = 4$, $N_{\ell_\Re} = 1$, $\tilde{N}_{\tilde{\ell}_\Re} = 2$ and $N_{\ell_\Im} = \tilde{N}_{\tilde{\ell}_\Im} = 2$, the term η_{F-QSM} can be expressed as follows:

$$\eta_{F-QSM} = \begin{cases} \left|S_\Re - \tilde{S}_\Re\right|^2 + 2\left|S_\Im - \tilde{S}_\Im\right|^2 + |S_\Re|^2 \\ \qquad \text{if } \gamma\left(\ell_\Re, \tilde{\ell}_\Re\right) = 1, \ \gamma\left(\ell_\Im, \tilde{\ell}_\Im\right) = 0 \\ 2\left|S_\Im - \tilde{S}_\Im\right|^2 + |S_\Re|^2 + 2\left|\tilde{S}_\Re\right|^2 \\ \qquad \text{if } \gamma\left(\ell_\Re, \tilde{\ell}_\Re\right) = 3, \ \gamma\left(\ell_\Im, \tilde{\ell}_\Im\right) = 0 \\ \left|S_\Re - \tilde{S}_\Re\right|^2 + \left|S_\Im - \tilde{S}_\Im\right|^2 + \left|\tilde{S}_\Re\right|^2 + |S_\Im|^2 + \left|\tilde{S}_\Im\right|^2 \\ \qquad \text{if } \gamma\left(\ell_\Re, \tilde{\ell}_\Re\right) = 1, \ \gamma\left(\ell_\Im, \tilde{\ell}_\Im\right) = 2 \\ \left|S_\Im - \tilde{S}_\Im\right|^2 + |S_\Re|^2 + 2\left|\tilde{S}_\Re\right|^2 + |S_\Im|^2 + \left|\tilde{S}_\Im\right|^2 \\ \qquad \text{if } \gamma\left(\ell_\Re, \tilde{\ell}_\Re\right) = 3, \ \gamma\left(\ell_\Im, \tilde{\ell}_\Im\right) = 2 \\ \left|S_\Re - \tilde{S}_\Re\right|^2 + \left|\tilde{S}_\Re\right|^2 + 2|S_\Im|^2 + 2\left|\tilde{S}_\Im\right|^2 \\ \qquad \text{if } \gamma\left(\ell_\Re, \tilde{\ell}_\Re\right) = 1, \ \gamma\left(\ell_\Im, \tilde{\ell}_\Im\right) = 4 \\ |S_\Re|^2 + 2\left|\tilde{S}_\Re\right|^2 + 2|S_\Im|^2 + 2\left|\tilde{S}_\Im\right|^2 \\ \qquad \text{if } \gamma\left(\ell_\Re, \tilde{\ell}_\Re\right) = 3, \ \gamma\left(\ell_\Im, \tilde{\ell}_\Im\right) = 4 \end{cases} \tag{55}$$

Example 3: when $N_t = 4$, $N_{\ell_\Re} = \tilde{N}_{\tilde{\ell}_\Re} = 2$ and $N_{\ell_\Im} = \tilde{N}_{\tilde{\ell}_\Im} = 2$, the term η_{F-QSM} can be expressed as follows:

$$\eta_{F-QSM} = \begin{cases} 2\left|S_\Re - \tilde{S}_\Re\right|^2 + 2\left|S_\Im - \tilde{S}_\Im\right|^2 \\ \quad if\ \gamma\left(\ell_\Re, \tilde{\ell}_\Re\right) = 0,\ \gamma\left(\ell_\Im, \tilde{\ell}_\Im\right) = 0 \\ 2\left|S_\Re - \tilde{S}_\Re\right|^2 + \left|S_\Im - \tilde{S}_\Im\right|^2 + |S_\Im|^2 + \left|\tilde{S}_\Im\right|^2 \\ \quad if\ \gamma\left(\ell_\Re, \tilde{\ell}_\Re\right) = 0,\ \gamma\left(\ell_\Im, \tilde{\ell}_\Im\right) = 2 \\ 2\left|S_\Re - \tilde{S}_\Re\right|^2 + 2|S_\Im|^2 + 2\left|\tilde{S}_\Im\right|^2 \\ \quad if\ \gamma\left(\ell_\Re, \tilde{\ell}_\Re\right) = 0,\ \gamma\left(\ell_\Im, \tilde{\ell}_\Im\right) = 4 \\ 2\left|S_\Im - \tilde{S}_\Im\right|^2 + \left|S_\Re - \tilde{S}_\Re\right|^2 + |S_\Re|^2 + \left|\tilde{S}_\Re\right|^2 \\ \quad if\ \gamma\left(\ell_\Re, \tilde{\ell}_\Re\right) = 2,\ \gamma\left(\ell_\Im, \tilde{\ell}_\Im\right) = 0 \\ 2\left|S_\Im - \tilde{S}_\Im\right|^2 + 2|S_\Re|^2 + 2\left|\tilde{S}_\Re\right|^2 \\ \quad if\ \gamma\left(\ell_\Re, \tilde{\ell}_\Re\right) = 4,\ \gamma\left(\ell_\Im, \tilde{\ell}_\Im\right) = 0 \\ \left|S_\Re - \tilde{S}_\Re\right|^2 + \left|S_\Im - \tilde{S}_\Im\right|^2 + |S_\Re|^2 + \left|\tilde{S}_\Re\right|^2 \\ + |S_\Im|^2 + \left|\tilde{S}_\Im\right|^2 \\ \quad if\ \gamma\left(\ell_\Re, \tilde{\ell}_\Re\right) = 2,\ \gamma\left(\ell_\Im, \tilde{\ell}_\Im\right) = 2 \\ 2|S_\Re|^2 + 2\left|\tilde{S}_\Re\right|^2 + 2|S_\Im|^2 + 2\left|\tilde{S}_\Im\right|^2 \\ \quad if\ \gamma\left(\ell_\Re, \tilde{\ell}_\Re\right) = 4,\ \gamma\left(\ell_\Im, \tilde{\ell}_\Im\right) = 4 \end{cases} \tag{56}$$

As stated earlier, QSM is considered a special case of the proposed F-QSM (54). This observation, without a doubt, manifests the principle of operation of the proposed F-QSM.

Following the same procedure, various examples of the transmission principle of the proposed F-QSM can be obtained and generalized to obtain the formula in (53).

B. COMPUTATIONAL COMPLEXITY ANALYSIS

The receiver's computational complexity of the different SMTs is determined by calculating the total number of real operations (TNRO) required at their ML decoders. It should be noted here that each complex multiplication requires four real multiplications. Therefore, in the case of the ML decoder of the conventional SM [8], calculating $\sum_{i=1}^{N_r} \|\boldsymbol{y_i} - \boldsymbol{h}_{li}S\|^2$ requires one complex multiplication (i.e., 4 real multiplications) to calculate $\boldsymbol{h}_{li}S$, and it further requires 4 real multiplications to calculate the square norm. However, these operations are repeated over the cardinality of $(2)^{R_{SM}}$ for each N_r value. Therefore, the TNRO required at the ML decoder of the conventional SM is given by

$$TNRO_{SM} = 8N_r\,(2)^{R_{SM}}\,. \tag{57}$$

Likewise, the computational complexity of the ML decoder of the conventional GSM can be determined. However, it should be noted here that GSM differs from the conventional SM approach in the manner of calculating $\boldsymbol{h}_{li}$. Calculating $\boldsymbol{h}_{li}$ in the ML decoder of the conventional GSM requires $N_u - 1$ complex summations [14], which requires $2(N_u - 1)$ real summations. Therefore, the TNRO of the ML decoder of the conventional GSM is given by

$$TNRO_{GSM} = 8N_r\,(2(N_u - 1))\,(2)^{R_{GSM}}\,. \tag{58}$$

In the proposed F-GSM [36], calculating $\boldsymbol{h}_{li}$ is different from both the conventional SM and GSM since it requires at maximum $\left(\left\lceil \frac{N_t}{2} - 1 \right\rceil\right)$ complex summations for all $N_t \geq 3$. Therefore, the TNRO of the ML decoder of the proposed F-GSM can be expressed as follows:

$$TNRO_{F-GSM} = 8N_r\left(\left\lceil 2\frac{N_t}{2} - 1 \right\rceil\right)(2)^{R_{F-GSM}}\,. \tag{59}$$

In the case of conventional QSM, the TNRO of its ML decoder is expressed as [18] as follows:

$$TNRO_{QSM} = 8N_r\,(2)^{R_{QSM}}\,. \tag{60}$$

However, the proposed F-QSM [38] is similar to the proposed F-GSM method, since calculating $\boldsymbol{h}_{\ell_\Re i}$ or $\boldsymbol{h}_{\ell_\Im i}$ requires at maximum $\left(\left\lceil \frac{N_t}{2} - 1 \right\rceil\right)$ complex summations for all $N_t \geq 3$. Therefore, the TNRO of the ML decoder of the proposed F-QSM can be expressed as follows:

$$TNRO_{F-QSM} = 8N_r\left(2\frac{N_t}{2} - 1\right)(2)^{R_{F-QSM}}\,. \tag{61}$$

It is worth mentioning that unlike the computational complexity of the conventional SMTs, the computational complexity of the proposed F-GSM and F-QSM is proportional to the number of transmit antennas. The logic behinds this is that the number of real summations required to calculate $\boldsymbol{h}_{li}$, $\boldsymbol{h}_{\ell_\Re i}$ or $\boldsymbol{h}_{\ell_\Im i}$ at the ML decoders of the F-GSM and the F-QSM are considered. However, in most of the current studies concerning the computational complexity analysis of SMTs, this number of operations is neglected [21].

VI. SIMULATION RESULTS

In this section, the performance of the proposed F-GSM and F-QSM is evaluated analytically and via comprehensive Monte Carlo simulations using a variety of system metrics. First, the achievable data rates of the proposed F-GSM and F-QSM are analyzed at different number of N_t and weighted against the achievable data rates of the conventional SM [8], GSM [14], and QSM [18]. Second, the ABER performance of the proposed schemes is evaluated analytically and via numerical simulations and compared with the ABER of the conventional SMTs under different MIMO configurations. Finally, the computational complexity of F-GSM and F-QSM is analyzed and weighted against the computational complexity of the different SMTs.

A. ACHIEVABLE DATA RATE

In what follows, the maximum achievable data rate under infinite SNR values of the proposed F-GSM (11) and F-QSM (15) are evaluated under different number of N_t and weighted against the maximum achievable data rate of SM, GSM, and

QSM provided by (2), (4), and (6), respectively. Unless stated otherwise, all the considered schemes are assumed to employ 4-QAM modulation on their TX sides. Moreover, the number of N_u used in conventional GSM is assumed to be equal to 2. Choosing $N_u = 2$ is for the reason that the error performance of the conventional GSM is degraded by increasing N_u since increasing N_u increases the possibility of having the same antenna index in the different antenna subsets [14].

The results of comparison are depicted in Fig. 3. As shown in Fig. 3, the proposed F-GSM and F-QSM provide a linear increment in their achievable data rates with respect to N_t, whereas conventional SM and QSM provide a logarithmic increment in their achievable data rates with respect to N_t. Moreover, the achievable data rate of the conventional GSM increases logarithmically with the combination of N_t and N_u. Hence, for $N_t = 16$, F-QSM and F-GSM attain SEs of 32 bpcu and 17 bpcu, respectively, whereas SM, GSM, and QSM achieve only 6 bpcu, 8 bpcu, and 10 bpcu, respectively. Therefore, the proposed schemes can provide a higher value of SE compared to the inferior SE values provided by the conventional SMTs.

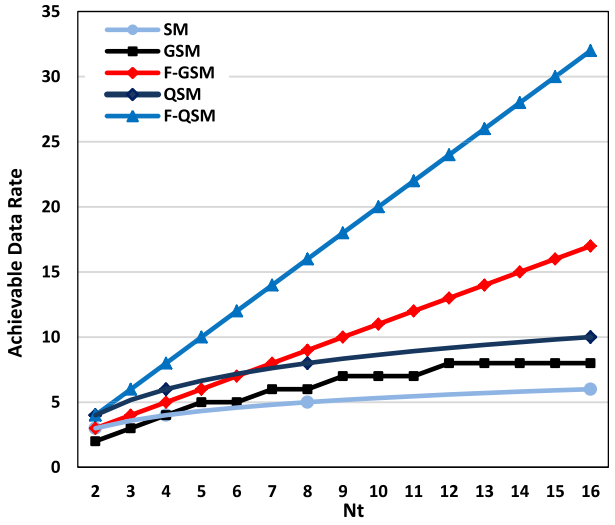

FIGURE 3. The maximum achievable data rates of the proposed F-GSM and F-QSM approaches compared to the maximum achievable data rates of SM [8], GSM [14], and QSM [18] at infinite SNR values.

B. ABER PERFORMANCE

In the following, the ABER performance of the proposed F-GSM and F-QSM is evaluated analytically and by using numerical simulations. As such, the values of $\eta_{F-GSM}(49)$ and $\eta_{F-QSM}(53)$ are used with (19) and (39) to obtain the upper-bound ABER using the union bounding technique. However, in the conventional SM, GSM, and QSM the values of $\eta_{SM}(42)$, $\eta_{GSM}(43)$, and $\eta_{QSM}(48)$ are also used with (19) and (39) to obtain the upper bound ABER of the conventional SM, GSM, and QSM, respectively. The analytical results are then substantiated using Monte Carlo simulations, in which each BER value is evaluated by averaging at least 10^6 symbol transmissions over the uncorrelated Rayleigh fading channel.

Herein, the channel parameters are assumed to be independent and identically distributed (i.i.d) complex Gaussian RVs with zero mean and unity variance as [14] and [18].

To compare meaningfully, in all the considered schemes, the transmitted energy is divided among all the active transmit antennas. Therefore, the transmitted energies in all the considered schemes are equal. As such, two different scenarios with different MIMO configuration are assumed. In the first scenario, all the considered schemes are assumed to employ the same modulation order, while they employ different number of transmit antennas to achieve an SE of 8 bpcu, 9 bpcu, and 10 bpcu, respectively. In the second scenario, all the considered schemes are assumed to employ the same number of transmit antennas, while they use different modulation orders to achieve an SE of 8 bpcu, 9 bpcu, and 10 bpcu, respectively.

1) SCENARIO 1: DIFFERENT NUMBER OF TRANSMIT ANTENNAS AND THE SAME MODULATION ORDER

Fig. 4, Fig. 5, and Fig. 6 depict the ABER of the proposed F-GSM and the F-QSM weighted against the ABER of conventional SM, GSM, and QSM for 8 bpcu, 9 bpcu, and 10 bpcu SEs, respectively. As stated before, all the considered schemes are assumed to use the same modulation order, whereas they use different transmit and receive antenna configurations to fulfill the aforementioned SEs. In Fig. 4, to achieve 8 bpcu SE, transmit and receive antenna configurations of 64×4, 12×4, 8×4, 7×4, and 4×4 are utilized in SM, GSM, QSM, F-GSM and F-QSM, respectively. However, all the considered schemes are assumed to employ 4-QAM modulation on their TX sides.

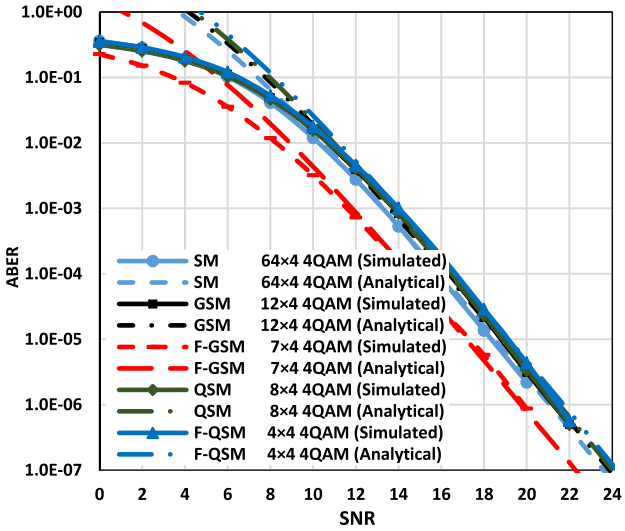

FIGURE 4. The ABER of the proposed F-GSM and F-QSM methods compared to the ABER of the SM [8], GSM [14], and QSM [18] for 8 bpcu transmission scenario 1.

As depicted in Fig. 4, the analytical results show a high consistency with the simulation results obtained for all the considered schemes for the pragmatic SNR values. However, at the low SNR values, the analytical results reveal

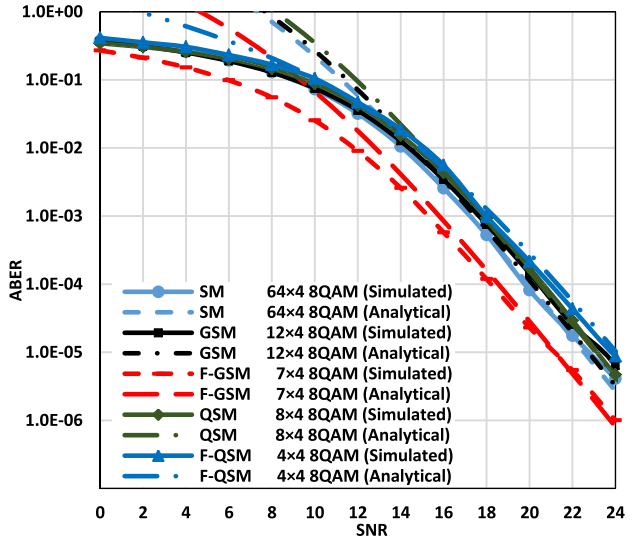

FIGURE 5. The ABER of the proposed F-GSM and F-QSM approaches compared to the ABER of SM [8], GSM [14], and QSM [18] for 9 bpcu transmission scenario 1.

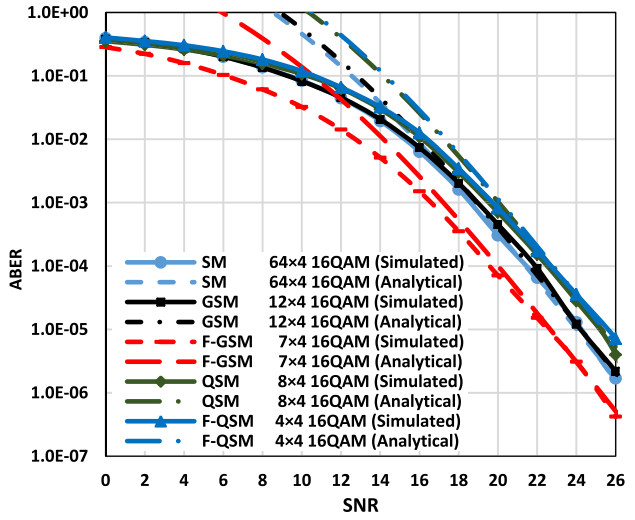

FIGURE 6. The ABERs of the proposed F-GSM and F-QSM approaches compared to the ABERs of SM [8], GSM [14], and QSM [18] for 10 bpcu transmission scenario 1.

a slight mismatch to the simulation results obtained for all the considered schemes. In other words, the upper bound is loose to the simulation results at low SNR values, but it tightens to the simulation results at the pragmatic SNR values. This is in accordance with other obtained results using similar bound as in [14], [18], and [21]. Moreover, the simulation results manifest that the proposed F-GSM exhibits significantly better BER performance than the conventional modulation schemes. However, the proposed F-QSM exhibits the same BER performance of the conventional modulation schemes. More specifically, the proposed F-GSM provides approximately 1.4 dB over the conventional SM and GSM, whereas it provides approximately 1.8 dB over the QSM.

Likewise, Fig. 5 depicts the ABER comparison for 9 bpcu SE, where all the considered schemes are assumed to employ 8-QAM modulation instead of 4-QAM modulation. Again, the simulation results manifest a close match to the analytical formulas for the pragmatic SNR values. Furthermore, the F-GSM provides approximately 1.8 dB over the SM and GSM, while it provides approximately 2.4 dB over the QSM.

In Fig. 6, the ABERs of the proposed schemes are compared to the ABERs of the conventional schemes for 10 bpcu SE, where all the considered schemes are assumed to employ 16-QAM modulation. As depicted in Fig. 6, the proposed F-GSM provides approximately 2 dB over the conventional SM and GSM, while it provides approximately 3 dB over the QSM.

This scenario demonstrates that the proposed F-GSM exhibits significantly better BER performance than all the considered schemes. This results from the potency of varying the number of transmit antennas (i.e., using different channel paths) in the proposed F-GSM compared to all the conventional schemes.

2) SCENARIO 2: THE SAME NUMBER OF TRANSMIT ANTENNAS AND DIFFERENT MODULATION ORDER

Fig. 7, Fig. 8, and Fig. 9 depict the ABER comparison for the second scenario in order to achieve 8 bpcu, 9 bpcu, and 10 bpcu SEs, respectively. In this scenario, all the considered schemes are assumed to employ the same transmit and receive antenna configurations while use different modulation orders to fulfill the aforementioned SEs. In Fig. 7, to fulfill 8 bpcu SE, 4×4 transmit and receive antenna configuration is used in all the considered schemes. Therefore, a modulation of 64-QAM is used with SM and GSM, whereas 32-QAM, 16-QAM, and 4-QAM are used in F-GSM, QSM, and F-QSM, respectively.

As depicted in Fig. 7, again, the simulation results are very akin to the analytical formulas at the pragmatic SNR values. Moreover, in this scenario the simulation results

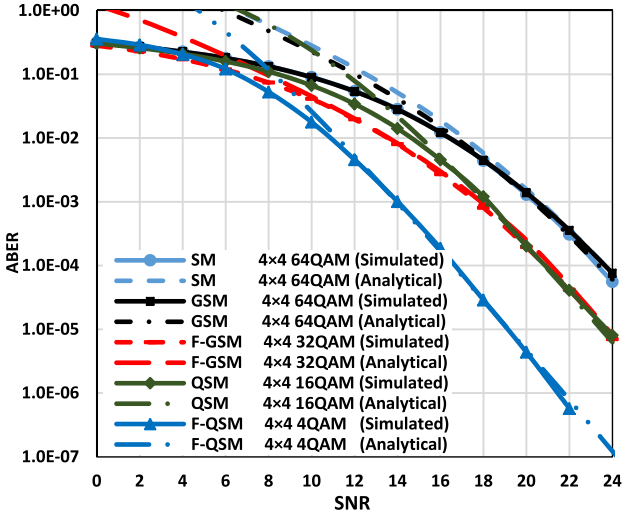

FIGURE 7. The ABERs of the proposed F-GSM and F-QSM methods compared to the ABERs of SM [8], GSM [14], and QSM [18] for 8 bpcu transmission scenario 2.

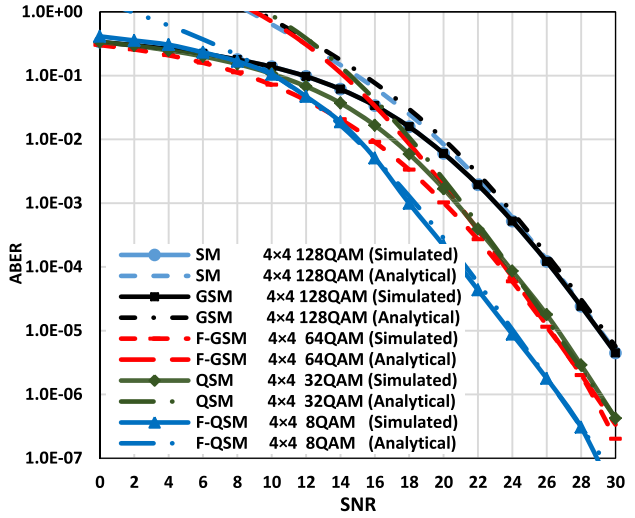

FIGURE 8. The ABERs of the proposed F-GSM and F-QSM methods compared to the ABERs of SM [8], GSM [14], and QSM [18] for 9 bpcu transmission scenario 2.

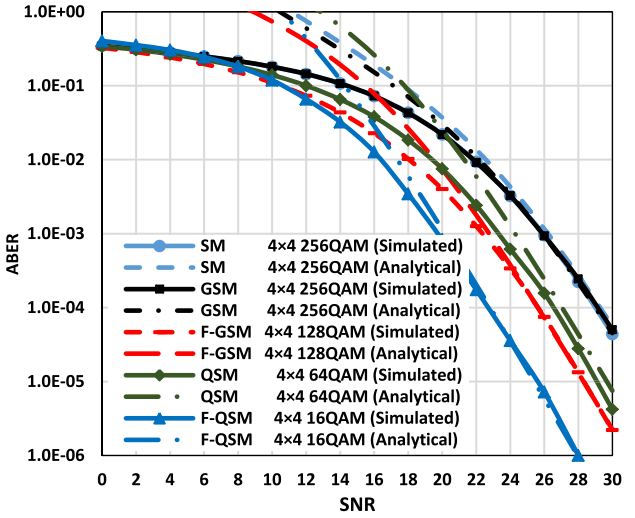

FIGURE 9. The ABERs of the proposed F-GSM and F-QSM methods compared to the ABERs of SM [8], GSM [14], and QSM [18] for 10 bpcu transmission scenario 2.

further manifest the superiority of the proposed F-GSM and F-QSM compared to the other SMTs. More specifically, the F-GSM provides approximately 2 dB over the conventional SM and GSM. However, it exhibits the same BER performance of the conventional QSM. Furthermore, the F-QSM provides approximately 6 dB over the conventional SM and GSM, while it provides approximately 4 dB over the QSM.

Similarly, Fig. 8 depicts the ABER comparison for 9 bpcu transmission, where 128-QAM modulation is used with SM and GSM, whereas 64-QAM, 32-QAM, and 8-QAM are used in the F-GSM, QSM and F-QSM, respectively. As shown in Fig. 8, F-GSM provides approximately 2.2 dB over conventional SM and GSM. However, it exhibits the same BER performance of the QSM. Moreover, the proposed F-QSM provides approximately 5 dB over the conventional SM and GSM, whereas it provides 3 dB over the QSM.

Fig. 9 depicts the ABER comparison for 10 bpcu SE, where 256-QAM modulation is used with SM and GSM, whereas 128-QAM, 64-QAM, and 16-QAM are used in the F-GSM, QSM, and F-QSM, respectively. As depicted in Fig. 9, the F-GSM provides approximately 3.8 dB over the SM and GSM. However, it exhibits the same BER performance of the QSM. Moreover, F-QSM provides approximately 5.6 dB over SM and GSM, while it provides approximately 2.8 dB over QSM.

This scenario concludes that the proposed F-QSM exhibits significantly better BER performance than all the considered schemes. This dates to the using of lower modulation order in the proposed F-QSM compared to all the considered schemes.

C. COMPUTATIONAL COMPLEXITY

In what follows, the computational complexity (i.e., TNRO) of the ML decoders of the proposed F-GSM and F-QSM is evaluated using (59) and (61), respectively and weighted against the computational complexity of the ML decoders of the SM, GSM, and QSM provided by (57), (58), and (60), respectively. To compare meaningfully, the computational complexity of all considered schemes is evaluated under the same SE (e.g., 8 bpcu SE is assumed). Herein, the comparison is evaluated using the parameters listed in TABLE 3 and the result of comparison is depicted in Fig. 10.

TABLE 3. Computational complexity of the different SMTS at 8 BPCU.

Modulation Technique	*SM*	*GSM*	*F-GSM*	*QSM*	*F-QSM*
$N_t \times N_r$	4×4	4×4	4×4	4×4	4×4
Modulation Order	64QAM	64QAM	32QAM	16QAM	4QAM
TNRO	8192	16384	16384	8192	16384

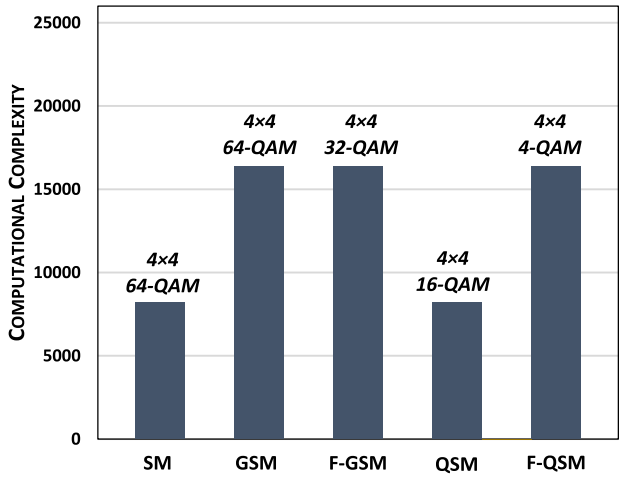

FIGURE 10. The Computational complexity of the proposed F-GSM and F-QSM compared to the computational complexity of the SM [8], GSM [14], and QSM [18] for 8 bpcu transmission.

As shown in Fig. 10, the proposed F-GSM and F-QSM exhibit the same computational complexity of the conventional GSM, while they exhibit a higher computational complexity than the conventional SM and QSM. The reason behinds this is due to the number of real summations required to calculate $\boldsymbol{h}_{li}$, $\boldsymbol{h}_{\ell_{\Re}i}$ or $\boldsymbol{h}_{\ell_{\Im}i}$ at the ML decoders of the proposed F-GSM and F-QSM.

VII. CONCLUSION

In this paper, the F-GSM and the F-QSM are proposed for sake of vanquishing the strict criticism of the conventional SMTs that constrains the data rate increment to be proportional to the base-two logarithm of the number of transmit antennas. Inspired by the concept of SM, the proposed schemes use an innovative method to embed additional information than the conventional SMTs. In particular, the proposed schemes differ from the traditional SMTs in the method of selecting the transmit antennas for data transmission. More specifically, in the proposed schemes, the number of transmit antennas varies from the state in which only one transmit antenna is activated to the state in which multiple/all transmit antennas are activated. Therefore, a linear increase between the achievable data rates of the proposed schemes and the number of transmit antennas is acquired. Moreover, in this paper, a general mathematical framework for assessing the ABER performance of different SMTs was developed. The proposed framework is protruded as the first major attempt that generalizes the analytical analysis of the different SMTs. In addition, the computational complexity of the proposed schemes was analyzed and compared with the computational complexity of the different SMTs. The simulation results corroborated the effectiveness of the conducted analysis by showing a high consistency with all the obtained formulas for the pragmatic range of SNR values.

ACKNOWLEDGMENT

The authors would like to express their gratitude to King Khalid University, Saudi Arabia for providing administrative and technical support.

REFERENCES

[1] E. Başar, Ü. Aygölü, and E. Panayırcı, "A new technique for OFDM: OFDM-index modulation," in *Proc. Signal Process. Commun. Appl. Conf. (SIU)*, Apr. 2013, pp. 1–4.
[2] E. Başar, U. Aygölü, E. Panayırcı, and H. V. Poor, "Orthogonal frequency division multiplexing with index modulation," *IEEE Trans. Signal Process.*, vol. 61, no. 22, pp. 5536–5549, Nov. 2013.
[3] E. Başar, "Multiple-input multiple-output OFDM with index modulation," *IEEE Signal Process. Lett.*, vol. 22, no. 12, pp. 2259–2263, Dec. 2015.
[4] E. Başar, "On multiple-input multiple-output OFDM with index modulation for next generation wireless networks," *IEEE Trans. Signal Process.*, vol. 64, no. 15, pp. 3868–3878, Aug. 2016.
[5] J. Jeganathan, A. Ghrayeb, L. Szczecinski, and A. Ceron, "Space shift keying modulation for MIMO channels," *IEEE Trans. Wireless Commun.*, vol. 8, no. 7, pp. 3692–3703, Jul. 2009.
[6] M. Di Renzo and H. Haas, "Space shift keying (SSK) modulation with partial channel state information: Optimal detector and performance analysis over fading channels," *IEEE Trans. Commun.*, vol. 58, no. 11, pp. 3196–3210, Nov. 2010.
[7] M. Di Renzo and H. Haas, "Space shift keying (SSK—) MIMO over correlated Rician fading channels: Performance analysis and a new method for transmit-diversity," *IEEE Trans. Commun.*, vol. 59, no. 1, pp. 116–129, Jan. 2011.
[8] R. Y. Mesleh, H. Haas, S. Sinanovic, C. W. Ahn, and S. Yun, "Spatial modulation," *IEEE Trans. Veh. Technol.*, vol. 57, no. 4, pp. 2228–2241, Jul. 2008.
[9] J. Jeganathan, A. Ghrayeb, and L. Szczecinski, "Spatial modulation: Optimal detection and performance analysis," *IEEE Commun. Lett.*, vol. 12, no. 8, pp. 545–547, Aug. 2008.
[10] M. Di Renzo, H. Haas, and P. M. Grant, "Spatial modulation for multiple-antenna wireless systems: A survey," *IEEE Commun. Mag.*, vol. 49, no. 12, pp. 182–191, Dec. 2011.
[11] M. Di Renzo, H. Haas, A. Ghrayeb, S. Sugiura, and L. Hanzo, "Spatial modulation for generalized MIMO: Challenges, opportunities, and implementation," *Proc. IEEE*, vol. 102, no. 1, pp. 56–103, Jan. 2014.
[12] J. Jeganathan, A. Ghrayeb, and L. Szczecinski, "Generalized space shift keying modulation for MIMO channels," in *Proc. IEEE Int. Symp. Pers., Indoor Mobile Radio Commun. (PIMRC)*, Sep. 2008, pp. 1–5.
[13] K. Ntontin, M. Di Renzo, A. I. Perez-Neira, and C. Verikoukis, "Adaptive generalized space shift keying," *EURASIP J. Wireless Commun. Netw.*, vol. 2013, no. 43, pp. 1–15, Feb. 2013.
[14] A. Younis, N. Serafimovski, R. Mesleh, and H. Haas, "Generalised spatial modulation," in *Proc. Asilomar Conf. Signals, Syst. Comput. (ASILOMAR)*, Nov. 2010, pp. 1498–1502.
[15] A. Younis, D. A. Basnayaka, and H. Haas, "Performance analysis for generalised spatial modulation," in *Proc. 20th Eur. Wireless Conf.*, 2014, pp. 1–6.
[16] T. Datta and A. Chockalingam, "On generalized spatial modulation," in *Proc. IEEE Wireless Commun. Netw. Conf. (WCNC)*, Apr. 2013, pp. 2716–2721.
[17] T. L. Narasimhan, P. Raviteja, and A. Chockalingam, "Generalized spatial modulation in large-scale multiuser MIMO systems," *IEEE Trans. Wireless Commun.*, vol. 14, no. 7, pp. 3764–3779, Jul. 2015.
[18] R. Mesleh, S. S. Ikki, and H. M. Aggoune, "Quadrature spatial modulation," *IEEE Trans. Veh. Technol.*, vol. 64, no. 6, pp. 2738–2742, Jun. 2015.
[19] M. M. Alwakeel, "Quadrature spatial modulation performance analysis over Rician fading channels," *J. Commun.*, vol. 11, no. 3, pp. 249–254, 2016.
[20] R. Mesleh and S. S. Ikki, "On the impact of imperfect channel knowledge on the performance of quadrature spatial modulation," in *Proc. IEEE Wireless Commun. Netw. Conf. (WCNC)*, Mar. 2015, pp. 534–538.
[21] R. Mesleh, S. S. Ikki, and H. M. Aggoune, "Quadrature spatial modulation–performance analysis and impact of imperfect channel knowledge," *Trans. Emerg. Telecommun. Technol.*, vol. 28, no. 1, p. e2905, 2017.
[22] O. Hiari and R. Mesleh, "A reconfigurable SDR transmitter platform architecture for space modulation MIMO techniques," *IEEE Access*, vol. 5, pp. 24214–24228, 2017.
[23] J. Li, M. Wen, X. Cheng, Y. Yan, S. Song, and M. H. Lee, "Generalized precoding-aided quadrature spatial modulation," *IEEE Trans. Veh. Technol.*, vol. 66, no. 2, pp. 1881–1886, Feb. 2017.
[24] R. Mesleh, S. Althunibat, and A. Younis, "Differential quadrature spatial modulation," *IEEE Trans. Commun.*, vol. 65, no. 9, pp. 3810–3817, Sep. 2017.
[25] M. Mohaisen, "Increasing the minimum Euclidean distance of the complex quadrature spatial modulation," *IET Commun.*, vol. 12, pp. 854–860, Apr. 2018.
[26] S. Althunibat and R. Mesleh, "Enhancing spatial modulation system performance through signal space diversity," *IEEE Commun. Lett.*, vol. 22, no. 6, pp. 1136–1139, Jun. 2018.
[27] S. Althunibat and R. Mesleh, "A bit-to-symbol mapping scheme for spatial modulation with partial channel state information," *IEEE Commun. Lett.*, vol. 21, no. 5, pp. 995–998, May 2017.
[28] E. Başar, M. Wen, R. Mesleh, M. Di Renzo, Y. Xiao, and H. Haas, "Index modulation techniques for next-generation wireless networks," *IEEE Access*, vol. 5, pp. 16693–16746, 2017.
[29] E. Başar, "Index modulation techniques for 5G wireless networks," *IEEE Commun. Mag.*, vol. 54, no. 7, pp. 168–175, Jul. 2016.
[30] R. Fan, Y. J. Yu, and Y. L. Guan, "Generalization of orthogonal frequency division multiplexing with index modulation," *IEEE Trans. Wireless Commun.*, vol. 14, no. 10, pp. 5350–5359, Oct. 2015.

[31] M. Wen, Y. Zhang, J. Li, E. Başar, and F. Chen, "Equiprobable subcarrier activation method for OFDM with index modulation," *IEEE Commun. Lett.*, vol. 20, no. 12, pp. 2386–2389, Dec. 2016.

[32] Y. Wu and W. Y. Zou, "Orthogonal frequency division multiplexing: A multi-carrier modulation scheme," *IEEE Trans. Consum. Electron.*, vol. 41, no. 3, pp. 392–399, Aug. 1995.

[33] S. Sugiura, T. Ishihara, and M. Nakao, "State-of-the-art design of index modulation in the space, time, and frequency domains: Benefits and fundamental limitations," *IEEE Access*, vol. 5, pp. 21774–21790, 2017.

[34] P. W. Wolniansky, G. J. Foschini, G. D. Golden, and R. A. Valenzuela, "V-BLAST: An architecture for realizing very high data rates over the rich-scattering wireless channel," in *Proc. URSI Int. Symp. Signals, Syst., Electron.*, Oct. 1998, pp. 295–300.

[35] A. Bhargave, R. J. P. de Figueiredo, and T. Eltoft, "A detection algorithm for the V-BLAST system," in *Proc. IEEE Global Telecommun. Conf. (GLOBECOM)*, Nov. 2001, pp. 494–498.

[36] M. Elsayed, H. S. Hussein, and U. S. Mohamed, "Fully generalised spatial modulation," in *Proc. 35th Nat. Radio Sci. Conf. (NRSC)*, Mar. 2018, pp. 274–282.

[37] H. Hussein, H. Esmaiel, and D. Jiang, "Fully generalised spatial modulation technique for underwater communication," *Electron. Lett.*, vol. 54, no. 14, pp. 907–909, 2018.

[38] H. S. Hussein and M. Elsayed, "Fully-quadrature spatial modulation," in *Proc. IEEE Int. Black Sea Conf. Commun. Netw. (BlackSeaCom)*, Jul. 2018, pp. 1–5.

[39] M. K. Simon and M.-S. Alouini, *Digital Communication Over Fading Channels*, vol. 95. Hoboken, NJ, USA: Wiley, 2005.

[40] J. G. Proakis, *Digital Communications*. New York, NY, USA: McGraw-Hill, 1995.

[41] R. Mesleh, O. Hiari, A. Younis, and S. Alouneh, "Transmitter design and hardware considerations for different space modulation techniques," *IEEE Trans. Wireless Commun.*, vol. 16, no. 11, pp. 7512–7522, Nov. 2017.

[42] O. S. Badarneh, S. Althunibat, R. Mesleh, and A. M. Magableh, "A unified performance analysis of decode-and-forward dual-hop relaying-based wireless energy harvesting with space modulation," *Trans. Emerg. Telecommun. Technol.*, vol. 29, p. e3419, Jul. 2018.

HANY S. HUSSEIN (M'13) received the B.E. degree in electrical engineering from South Valley University, Egypt, in 2004, the M.Sc. degree in communication and electronics engineering from South Valley University, Egypt, in 2009, and the Ph.D. degree in communication and electronics engineering from the Egypt-Japan University of Science and Technology, in 2013. In 2012, he was a Researcher Assistant with Kyushu University, Japan. He has been an Assistant Professor with the Faculty of Engineering, Aswan University, since 2013. Also, he has been with King Khalid University, Saudi Arabia, as an Assistant Professor, since 2018. His research interests include digital signal processing, blind signal separation, image and video processing, multimedia, image and video coding, low power wireless communication, 1-bit ADC multiple-input multiple-output, underwater communication, index modulation, and spatial modulation. He is a technical committee member of many international conferences and a reviewer of many international conferences, journals and transactions. He is the General Co-Chair of the IEEE ITCE' 2018.

MOHAMED ELSAYED (S'18) received the B.Sc. degree in electrical engineering from Sohag University, Sohag, Egypt, in 2014. He is currently pursuing the M.Sc. degree in electrical engineering with Assiut University, Assiut, Egypt. He currently serves as a Demonstrator with the Electrical Engineering Department, Sohag University. His research interests include multiple-input multiple-output systems, signal processing, wireless technology, wireless networks, index modulation, spatial modulation, OFDM, and cooperative communications. He has served as a TPC member of IEEE ISWC'18. He has received the Best Paper Award from the 35th National Radio Science Conference (NRSC2018).

USAMA SAYED MOHAMED received the B.Sc. and M.Sc. degrees from Assiut University, Assiut, Egypt, and the Ph.D. degree from Czech Technical University, Prague, Czech Republic, all in electrical engineering. From 1999 to 2000, he was a Research Assistant with the University of California at Santa Barbara, Santa Barbara, CA, USA. From 2001 to 2002, he was a Post-Doctoral Fellow with the Faculty of Engineering, Czech Technical University, Prague, Czech Republic. He is currently a Professor with the Faculty of Engineering, Assiut University. He was the Head of the Electrical Engineering Department and the Vice Dean of Graduate Studies and Research, Faculty of Engineering, Assiut University. He authored and co-authored more than 135 scientific papers. He has been selected for inclusion in the 2010 Edition of the 'USA-Marquis Who's Who in the World.' His research interests include signal processing, wireless technology, wireless networks, image coding, statistical signal processing, blind signal separation, and video coding.

HAMADA ESMAIEL received the B.E. degree in electrical engineering and the M.Sc. degree in wireless communications from South Valley University, Egypt, in 2005 and 2010, respectively, and the Ph.D. degree in communication engineering from the University of Tasmania, Australia, in 2015. In 2011, he was a Researcher Assistant with the Wireless Communication Laboratory, Wonkwang University, Iksan, South Korea. Since 2015, he has been an Assistant Professor with Aswan University, Egypt. His current research interests are 5G networks, Li-Fi technology, millimeter wave transmissions, underwater communication, and MIMO systems. He is the General Co-Chair of the IEEE IEEE ISWC'18. He is a technical committee member of many international conferences and a reviewer of many international conferences, journals, and transactions.

EHAB MAHMOUD MOHAMED received the B.E. degree in electrical engineering and the M.E. degree in computer science from South Valley University, Egypt, in 2001 and 2006, respectively, and the Ph.D. degree in information science and electrical engineering from Kyushu University, Japan, in 2012. From 2013 to 2016, he joined Osaka University, Japan, as a Specially Appointed Researcher. Since 2017, he has been an Associate Professor with Aswan University, Egypt. He joined Prince Sattam bin Abdulaziz University, Saudi Arabia, in 2018. He is the General Chair of IEEE ITEMS'16 and IEEE ISWC'18. He is a technical committee member of many international conferences and a reviewer of many international conferences, journals, and transactions. His current research interests are 5G networks, cognitive radio networks, millimeter wave transmissions, Li-Fi technology, MIMO systems, and underwater communication.